UNIVERSITÄT AUGSBURG
Universitätsbibliothek

OPEN ACCESS
OPUS AUGSBURG

Cascading continental-scale floods across Europe in 1342–1343

Andrea Kiss, Alberto Viglione, Mariano Barriendos, Silvia Enzi, Martin Bauch, Kris Decker, Nicolas Maughan, Dag Retsö, Astrid Ogilvie, Miriam Bertola, Tim Soens, Libor Elleder, Rudolf Brázdil, Kathleen Pribyl, Juraj Parajka, Ioannis Telelis, Inês Amorim, Josep Barriendos, Oliver Böhm, Gerardo Benito, Chiara Bertolin, Dario Camuffo, Denis Coeur, Gaston Demarée, Radoslaw Doktor, Markus Dotterweich, Rüdiger Glaser, Jürgen Komma, Neil Macdonald, Hrvoje Petrić, Christian Rohr, Petra Schmocker-Fackel, Lothar Schulte, Willem H. J. Toonen, Oliver Wetter, Günter Blöschl

Angaben zur Veröffentlichung / Publication details:

Kiss, Andrea, Alberto Viglione, Mariano Barriendos, Silvia Enzi, Martin Bauch, Kris Decker, Nicolas Maughan, et al. 2026. "Cascading continental-scale floods across Europe in 1342–1343." *Nature* 656: 638–45. https://doi.org/10.1038/s41586-026-10888-8.

Nutzungsbedingungen / Terms of use: **CC BY 4.0**

Dieses Dokument wird unter folgenden Bedingungen zur Verfügung gestellt: / This document is made available under these conditions:
CC-BY 4.0: Creative Commons: Namensnennung
Weitere Informationen finden Sie unter: / For more information see:
https://creativecommons.org/licenses/by/4.0/deed.de

Article

Cascading continental-scale floods across Europe in 1342–1343

https://doi.org/10.1038/s41586-026-10888-8

Received: 24 October 2024

Accepted: 6 July 2026

Published online: 12 August 2026

Open access

Check for updates

Andrea Kiss[1]✉, Alberto Viglione[2], Mariano Barriendos[3], Silvia Enzi[4], Martin Bauch[5], Kris Decker[6], Nicolas Maughan[7], Dag Retsö[8], Astrid Ogilvie[9,10], Miriam Bertola[1], Tim Soens[11], Libor Elleder[12], Rudolf Brázdil[13,14], Kathleen Pribyl[11,15], Juraj Parajka[1], Ioannis Telelis[16], Inês Amorim[17], Josep Barriendos[18], Oliver Böhm[19], Gerardo Benito[20], Chiara Bertolin[21], Dario Camuffo[4], Denis Coeur[22], Gaston Demarée[23], Radoslaw Doktor[24], Markus Dotterweich[25], Rüdiger Glaser[26], Jürgen Komma[1], Neil Macdonald[27], Hrvoje Petrić[28], Christian Rohr[29,30], Petra Schmocker-Fackel[31], Lothar Schulte[32], Willem H. J. Toonen[33], Oliver Wetter[29,34] & Günter Blöschl[1]✉

Europe has experienced extreme floods in recent decades. However, even larger floods are possible and must be considered in flood risk management[1,2]. Their characteristics can be clarified by analysing the largest documented historical floods. In Central Europe, the Magdalena Flood of July 1342 is usually considered the largest of the last millennium; however, knowledge of its characteristics is incomplete[3–7]. Here we show that 16 major flood events occurred across much of Europe between late 1341 and 1343. Four of these events had return periods of 500–1,000 years (the Magdalena, Bartholomew, Candlemas and Jacob Floods). Although Magdalena was thought previously to be the only extreme European flood in 1342[3,7], our new documentary dataset suggests that it formed part of a broader sequence. The year with the greatest number of extreme floods during the past 700 years was 1342, and 1343 ranks among the top ten. This highly unusual sequence of floods had substantial socio-economic impacts, including a paradigm shift in flood mitigation measures in Europe. A series of volcanic eruptions along with multi-annual Arctic sea ice retreat is a plausible cause of this flood sequence. Clusters of extreme floods occurring within a few months are rarely considered in risk management[8]. Quick and proactive risk strategies are needed that account for this eventuality.

Numerous major floods have occurred in recent decades[1,8], and their magnitude and frequency are increasing in many parts of Europe[2]. Defence against the impacts of such events include flood management measures, such as the building of levees and the implementation of land use planning. These measures are generally based on knowledge of events in the immediate past. However, it is possible that even larger floods than those in the recent times may occur, some of them in close sequence. The ability to evaluate the possibilities and consequences of such events will be enhanced by the analysis of flood events in the more distant past.

The Magdalena Flood in Europe

In Central Europe, the Magdalena Flood is usually considered to have been the largest flood in the last millennium, and the most severe single erosion event during the Holocene[3]. The flood peaked in the central

[1]Institute of Hydraulic Engineering and Water Resources Management, Vienna University of Technology, Vienna, Austria. [2]Department of Environment, Land and Infrastructure Engineering, Politecnico di Torino, Turin, Italy. [3]Institute of Environmental Assessment and Water Research (IDAEA-CSIC), Barcelona, Spain. [4]National Research Council of Italy, Institute of Atmospheric Sciences and Climate (CNR-ISAC), Padova, Italy. [5]Leibniz Institute for the History and Culture of Eastern Europe (GWZO), Leipzig, Germany. [6]Department of Cultural and Science Studies, University of Lucerne, Lucerne, Switzerland. [7]Environmental Sciences Department, Aix-Marseille University, Marseille, France. [8]Department of Economic History and International Relations, Stockholm University, Stockholm, Sweden. [9]Stefansson Arctic Institute, Akureyri, Iceland. [10]Institute of Arctic and Alpine Research (INSTAAR), University of Colorado, Boulder, CO, USA. [11]Centre for Urban History and the Urban Studies Institute, University of Antwerp, Antwerp, Belgium. [12]Czech Hydrometeorological Institute, Prague, Czech Republic. [13]Institute of Geography, Masaryk University, Brno, Czech Republic. [14]Global Change Research Institute, Czech Academy of Sciences, Brno, Czech Republic. [15]Climate Research Unit, University of East Anglia, Norwich, UK. [16]Research Center for Greek and Latin Literature, Academy of Athens, Athens, Greece. [17]Department of History and of Political and International Studies (CITCEM), University of Porto, Porto, Portugal. [18]Department of Geography, Autonomous University of Barcelona, Barcelona, Spain. [19]Institute of Geography, University of Augsburg, Augsburg, Germany. [20]National Museum of Natural Sciences, Spanish Research Council (CSIC), Madrid, Spain. [21]Norwegian University of Science and Technology, Trondheim, Norway. [22]ACTHYS-Diffusion, Grenoble, France. [23]Meteorological Research and Development Department, Royal Meteorological Institute of Belgium, Brussels, Belgium. [24]Centre for Flood and Drought Modelling, Institute of Meteorology and Water Management – National Research Institute, Warsaw, Poland. [25]GEOarch – Applied Geoarchaeology, Landau, Germany. [26]Institute of Physical Geography, University of Freiburg, Freiburg, Germany. [27]Department of Geography and Planning, School of Environmental Sciences, University of Liverpool, Liverpool, UK. [28]Department of History, Faculty of Humanities and Social Sciences, University of Zagreb, Zagreb, Croatia. [29]Institute of History, University of Bern, Bern, Switzerland. [30]Oeschger Centre for Climate Change Research, University of Bern, Bern, Switzerland. [31]Hydrology Division, Federal Office for the Environment (FOEN), Bern, Switzerland. [32]FluvAlps-PaleoRisk Research Group, Department of Geography, University of Barcelona, Barcelona, Spain. [33]Earth and Climate Cluster, Vrije Universiteit Amsterdam, Amsterdam, The Netherlands. [34]Present address: Institute of History, University of Bern, Bern, Switzerland. ✉e-mail: kiss@hydro.tuwien.ac.at; bloeschl@hydro.tuwien.ac.at

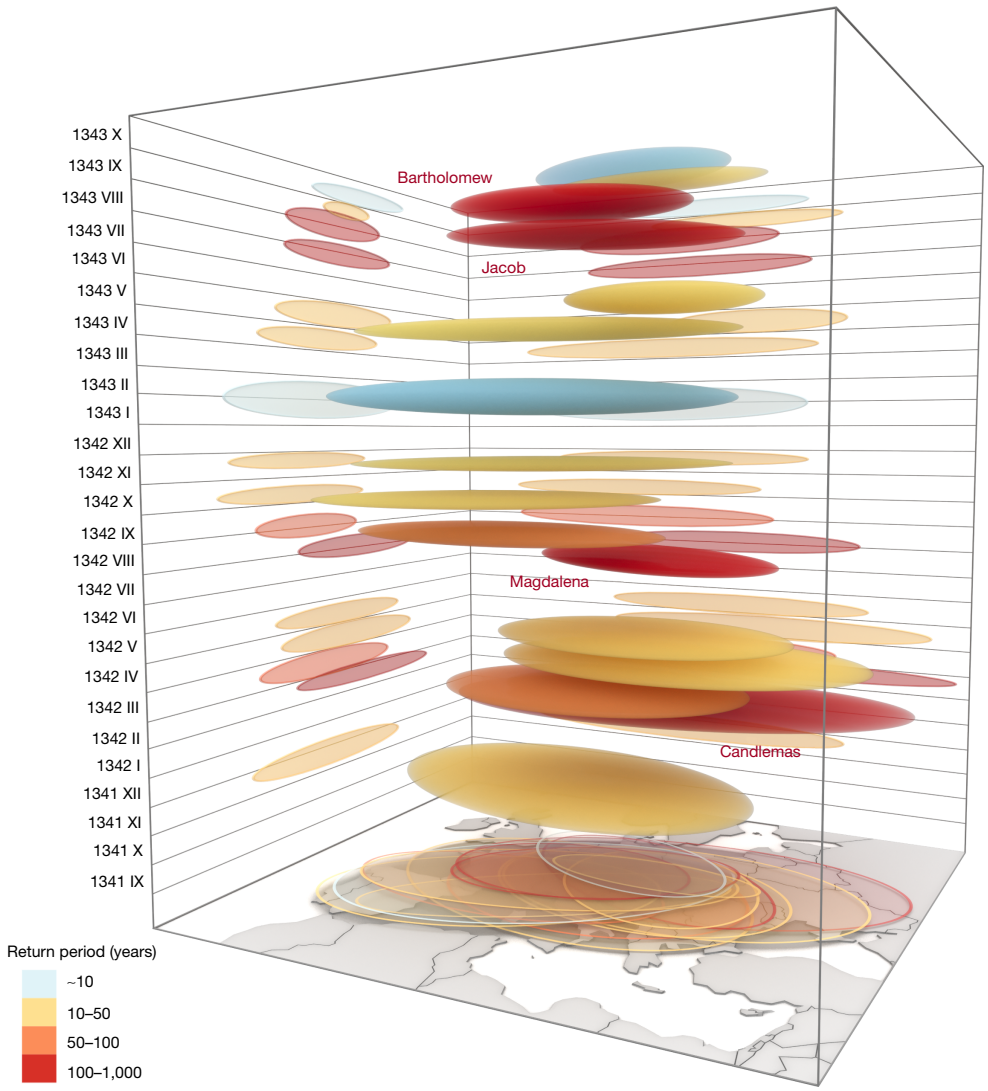

Fig. 1 | Conceptual reconstruction of the 1342–1343 floods in Europe. Sixteen events are rendered as ellipsoids based on historical evidence on floods (161 data points) and meteorological conditions (more than 217 data points), and on modern analogue events for spatial extent (Supplementary Data 1, 2, 4 and 5; Methods). Colours represent the severity of the events. For a dynamic visualization, see Supplementary Video 1.

part of the Holy Roman Empire (Germany) in late July 1342. Based on documentary records and soil erosion patterns, the return period of the driving precipitation was estimated as 10,000 years[4]. It was probably caused by an extensive Vb weather pattern, that is, one that transports atmospheric moisture from the Mediterranean into Central Europe[5]. Flood levels of the Rhine and Main rivers had return periods of between 100 and 1,000 years[6]. The losses were enormous, with thousands of fatalities, most bridges and the settlements along the main rivers destroyed and the agricultural damage caused dearth[7]. In Prague, a catastrophic flood occurred in February 1342[9] and, in the Carpathian Basin, the greatest annual number of floods of the Middle Ages were recorded in 1342[10].

However, so far, the exact magnitude, spatial extent, frequency and impact of the European floods during 1342 and 1343 remain unclear. The analysis presented here encompasses a new dataset on floods, weather extremes and socio-economic consequences collected from more than 1,000 original source entries and natural proxy evidence, to infer the flood characteristics in Europe during 1342–1343.

Flood and meteorological data

The data are based on the collation of published and manuscript chronicles, annals, economic and legal administrative records, a weather diary, scientific essays and private and official correspondence (Supplementary Data 1–3). To ensure reliability of the data, we use almost exclusively contemporary documentation written during or shortly after 1342–1343. Up until now, most of these data have not been used in flood and weather reconstructions.

Flood magnitudes are quantified by a standard three-scaled index of notable, great and outstanding floods[11] based on direct indicators, such as the level and spatial extent of flood waters relative to identifiable landmarks and, to a lesser extent, indirect indicators such as environmental or socio-economic impacts. For air temperature, precipitation and socio-economic consequences we use indices based on analogous indicators. Furthermore, the uncertainty (Supplementary Data 1 and 2) of the indices is quantified. These results are then compared with a historical flood dataset[11], extended in quantity and to cover the period 1300–2020 (Supplementary Data 4; Methods), and to instrumental flood data from 1960–2020[1,2].

Here we find that the year 1342 had the greatest number of great and outstanding floods reported in the past 700 years in Europe. The year 1343 was also an outstanding flood year. Within these two years, 16 major flood events occurred in Europe (Fig. 1, Extended Data Fig. 1 and Extended Data Tables 1 and 2), and four of these had return periods of 500–1,000 years. This finding contrasts

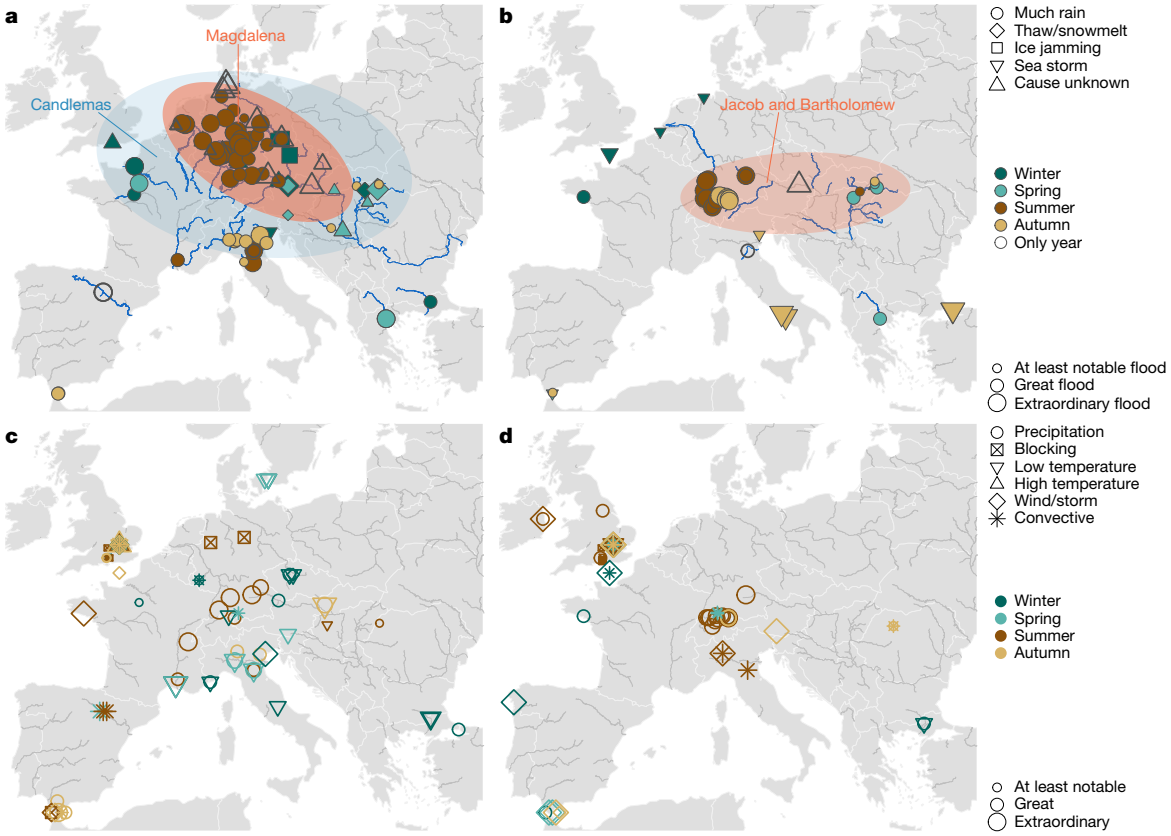

Fig. 2 | Spatiotemporal distribution of floods and weather information in 1342 and 1343. a,**b**, Locations of reported flooding and the affected principal rivers. Ellipses, spatial coverage of the four main floods indicated by documentary evidence in 1342 (**a**) and 1343 (**b**). **c**,**d**, Locations of reported weather events in 1342 (**c**) and 1343 (**d**). Symbol type, flood causes and weather phenomena; colours, seasons; symbol size, event intensity. For details, see Supplementary Data 1a and 2a.

with the previous understanding of only one extreme flood in this period.

String of pearls: the 1342–1343 floods

The autumn of 1341 was wet, with great mid-November and December floods in East Central and Southeast Europe (Figs. 1 and 2a,c, Extended Data Tables 1 and 2 and Supplementary Data 1 and 2). The subsequent cold and snowy winter and sudden thaw caused an outstanding flood in mid-February 1342 in Western and Central Europe (approximate return periods of T = 200–1,000 years) in Prague and along the Danube. We term this event the 'Candlemas Flood' after the Christian feast on 2 February (Julian calendar) mentioned by the sources. After three spring floods in Central, Western and Southeast Europe (T = 50–100 years) the extraordinary Magdalena Flood hit Southern Germany, in particular the Main catchment, in late July, traditionally on the day of Saint Maria Magdalena, with estimated flood return periods of 1,000–10,000 years[6]. This event was followed by a great late summer flood in Northern Italy (T = 50–100 years) and two autumn floods in the Mediterranean and the Carpathian Basin (T = 20–100 years).

The wet January and February of 1343 caused flooding in Western and Central Europe, followed by a Europe-wide wet spring with floods in Southeast Spain and the Carpathians (T = 10–100 years), and prolonged flooding in Northern Italy, the Carpathians and in the Balkans (Figs. 1 and 2b,d, Extended Data Tables 1 and 2 and Supplementary Data 1 and 2). In late July an outstanding flood (termed here the Jacob Flood; T = 100–1,000 years) affected primarily the northern and central Alps and the Carpathians, and in late August an even bigger flood (termed here the Bartholomew Flood; T = 200–1,000 years) affected the same area. In mid-September, a third event hit the tributaries of Lake Constance, and floods continued in the Carpathians in October (T = 10–100 years).

Short-term and long-term consequences

The 1342–1343 floods caused many thousands of direct fatalities in Europe and many more indirect fatalities caused by food shortages and disease (Fig. 3). Thus, for example, the Franciscan friar in Lindau, Johann von Winterthur, reported a two miles extension of the Candlemas Flood along the Danube and some 6,000 deaths: "ut fertur, et quod de hominibus VI milia absorbuit" (Supplementary Data 3). Concurrently, Venice was also inundated heavily. The Magdalena Flood destroyed most settlements and all bridges[7], roads and mills along the Middle Rhine, Main and its tributaries. The Jacob and Bartholomew Floods had the same effect along the Rhine from Schaffhausen to Basel, and so had the Candlemas Flood, especially along the Elbe and its tributaries. Even the iconic stone bridge across the Vltava in Prague, standing since 1172, was swept away. In fact, during these 2 years the bridges across the main European rivers were damaged, and roads on a continental scale were disrupted, which had a fundamental effect on European transportation and travel capabilities (Fig. 3 and Extended Data Table 3).

The repetitive, widespread and long-lasting flooding in these densely populated areas provoked fear and a feeling of emergency among the European population, given that relatively few floods had occurred in the previous decades (Supplementary Data 4)[12,13]. According to Johann von Winterthur, Paris astronomers suggested that this very unusual sequence of flooding happens only once every 500 years and attributed it to a specific stellar constellation[14]. According to the annalists in Stift Neuberg, Austria, the year 1342 seemed as if the 'four elements had been

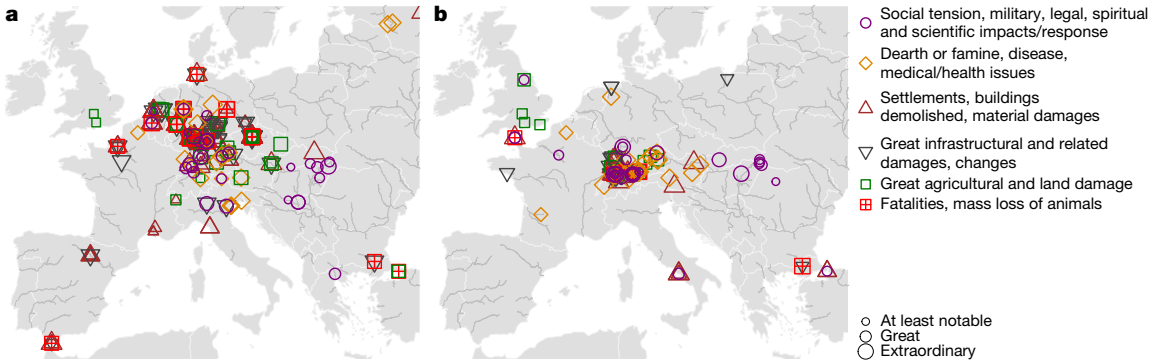

Fig. 3 | Socio-economic impacts of floods in 1342 and 1343. a,**b**, Data documented in 1342 (**a**) and 1343 (**b**). Symbol type, main group of impact type; symbol size, intensity of impact. For details, see Extended Data Table 4 and Supplementary Data 3.

disturbed all around the world' ("In toto universo in quatuor elementis diversis temporibus fuit confusio et disturbium") when 'floods caused numerous great losses' ("per inundacionem aquarum diversa dispensia provenerunt")[13]. These several floods caused the abandonment of village sites such as Stollhofen (today part of Traismauer) on the Danube in Lower Austria—a decision taken only rarely after a single flood (Supplementary Data 3).

Flood mitigation, dearth and banking crisis

These several floods also produced a paradigm shift in flood mitigation strategies across Europe. More robust bridges were made partly or entirely of stone (for example, in Prague, Dresden, Säckingen), stronger town walls were designed for flood protection (for example, in Strasbourg), river sections regulated and substantial dykes (for example, Danube at Oberaltaich, the River Nogat/Vistula near Gdansk) and riverside fortifications amenable to flood warning (for example, in Säckingen) were constructed (Extended Data Table 2, Fig. 3, Supplementary Data 3 and Supplementary Information sections 1 and 2). For example, the redesign of the Charles Bridge in Prague resulted in a more massive structure, with broader and higher arches, sharply pointed ice-breaking piers, and riverbanks elevated by up to 9 m—design choices that address directly the impacts of floodwater, ice and debris experienced in 1342 (Supplementary Information section 1).

During 1342–1344, lost harvests and transportation problems resulted in dearth and famine in much of Europe, particularly in Southern Germany, Switzerland and Austria, and food prices soared in Western and Central Europe (Fig. 3 and Supplementary Information section 3). Based on merchants' reports, the abbot of Saint-Martin de Tournai even suggested a 'worldwide' (that is, Europe-wide) dearth in 1342[13]. Very unusual salt production problems in Italy in 1342–1343, presumably caused by flooding of salt pans, led to imports from locations as far away as Cyprus, as evidenced by contemporary accounts noting that salt was produced everywhere only in 'small quantities' because of the 'weather conditions' ("cum isto anno [1342] propter condicionem temporis sal factus sit in modica quantitate in omni parte"; Supplementary Information section 3). Disruption of transportation routes hindered military operations (for example, siege of Algeciras, Byzantine civil war; Supplementary Data 1, 3) and, apart from other historical reasons[14], could also be a contributing factor to the economic turmoil and escalation of the great crisis in the Italian banking system from 1343[15] (Fig. 3, Supplementary Data 3 and Supplementary Information section 3).

In extensive areas, the flood waters did not recede between events, causing major multi-annual health problems. Thus, for example, in late 1344, the Hungarian archbishop and royal physician László Kaboli, living in Kalocsa by the Danube, died a few months after complaining to the pope about the 'unhealthy waters' ("quod terra, in qua Colocensis ecclesia situata existit, paludibus et diversi aquis immundis et fetidis circumdata")[16]. Water-borne diseases[17] such as the mortal 'bleeding illness' (presumably dysentery or another bloody diarrhoea) were reported in 1342–1343 in the flood- and famine-affected regions and beyond (Johann von Winterthur; Supplementary Data 3 and Supplementary Information section 3).

Most unusual flood biennium in 700 years

In context of the past 700 years, 1342 stands out as the year with the largest number of great and extraordinary floods in Europe, and 1343 is the third most important (Fig. 4). Although the major twentieth and twenty-first century floods happened more or less randomly in time, the fourteenth century floods were clustered in 1342–1343. The 16 flood events across Europe are reflected in 121 individual class 2 and 3 floods (Fig. 4). Some rivers were affected particularly often during these two years. The Main, Rhine, Danube and Tisza flooded at least three times in 1342, and the Rhine, Bodensee and Tisza at least two or three times in 1343 (Extended Data Table 1). The flood sequence of 1342–1343 is a model example of a more frequent than expected occurrence of mega-events[1,8].

Analogues: 1342–1343 and recent floods

To better understand the relevance of the 1342–1343 floods to present-day flood management, we placed them into the context of recent European floods. We chose analogue events in the last 60 years that were similar to the historical events in terms of affected area, runoff generation processes, seasonality and, where possible, flood magnitude (Fig. 5 and Extended Data Tables 1 and 2).

The Jacob and Bartholomew Floods show characteristics similar to those of some of the greatest twentieth century Vb-induced Central European floods (2005 and 1999, respectively), when much of the atmospheric moisture originated mainly from the Mediterranean[5] (Supplementary Information section 4). The similar characteristics were occurrence in summer, extreme precipitation over the northern Alps indicative of Vb storm tracks and sunshine in Scandinavia indicative of atmospheric blocking. The Magdalena flood exhibited elements of a Vb pattern, but with greater structural complexity, and showed similarities to the events of 2013 and 2021 (Supplementary Information section 4). However, the spatial extent of the Magdalena flood was much larger than that of the recent floods. The comparison shows that the 1342–1343 double flood year was truly extraordinary, as if the extreme 1999, 2002, 2005, 2006 and the 2013 great European flood events and a dozen of other 10- to 100-year return period floods had all happened within less than 2 years. In 1342–1343, more European scale outstanding floods occurred than in the previous 60 years, and they were mostly larger (Fig. 5). These return periods,

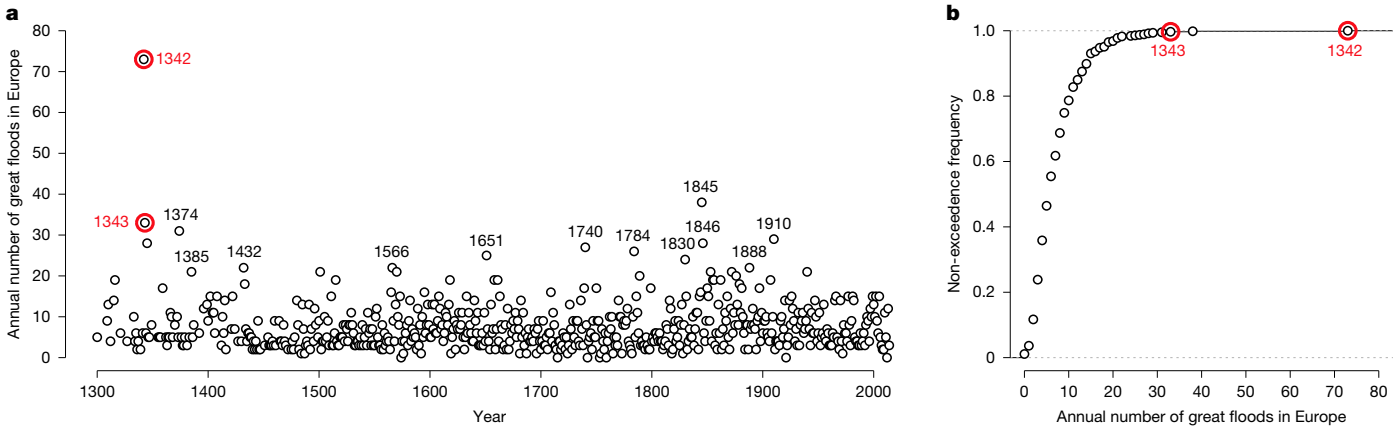

Fig. 4 | Annual frequency of great and extraordinary floods in Europe in the last 700 years. a, Time series. **b**, Associated frequency plot. Homogenized time series with bias correction of the sum of class 2 and 3 floods. In the context of the past 700 years, 1342 stands out as the year with the largest number of great and extraordinary floods in Europe. For similar plots without bias correction, see Extended Data Fig. 1. For details, see Supplementary Data 4.

presented in Fig. 5, are expert-based, subjective estimates, derived from documentary, archaeological and sedimentary water-level evidence.

The 1342–1343 period was also rather unusual in its flood timing. Along the Main and the Middle Rhine, the Magdalena Flood occurred in summer while the largest twentieth to twenty-first century floods occurred in winter or spring[11,18]. In August 1342, a major flood occurred in northern Italy at the Reno, but essentially all floods in the twentieth century have been in late autumn or winter.

Process causes: volcanoes and sea ice

The extraordinary magnitudes and frequency of the 1342–1343 floods are consistent with the low temperatures evidenced by tree-ring analysis[19,20] and a historically negative correlation between temperature and floods[11]. Although no direct causal explanation is yet possible based on the available climate models and simulations, our systematic analysis of documentary-based and high-resolution paleoclimate, terrestrial and extra-terrestrial evidence suggests that Arctic sea ice reduction, volcanic eruptions and related internal climate variability together could be responsible for the exceptional flood sequence.

Based on the Smithsonian Institution Global Volcanism Programme (GVP)[21], at least five tropical volcanoes (E-tr in Fig. 6)—including Pelée in the Caribbean for which the volcanic explosivity index (VEI) is 4—erupted around 1340, although their dating is uncertain. Ice-core analyses suggest a major tropical eruption between 1341 and 1345, reflected in global sulfate injection and Northern Hemisphere sulfate injection[22–24], as shown in Fig. 6 (Supplementary Information section 5.1). Out of the eight extratropical eruptions in 1340–1341, according to the GVP database, an unusually high number of five occurred

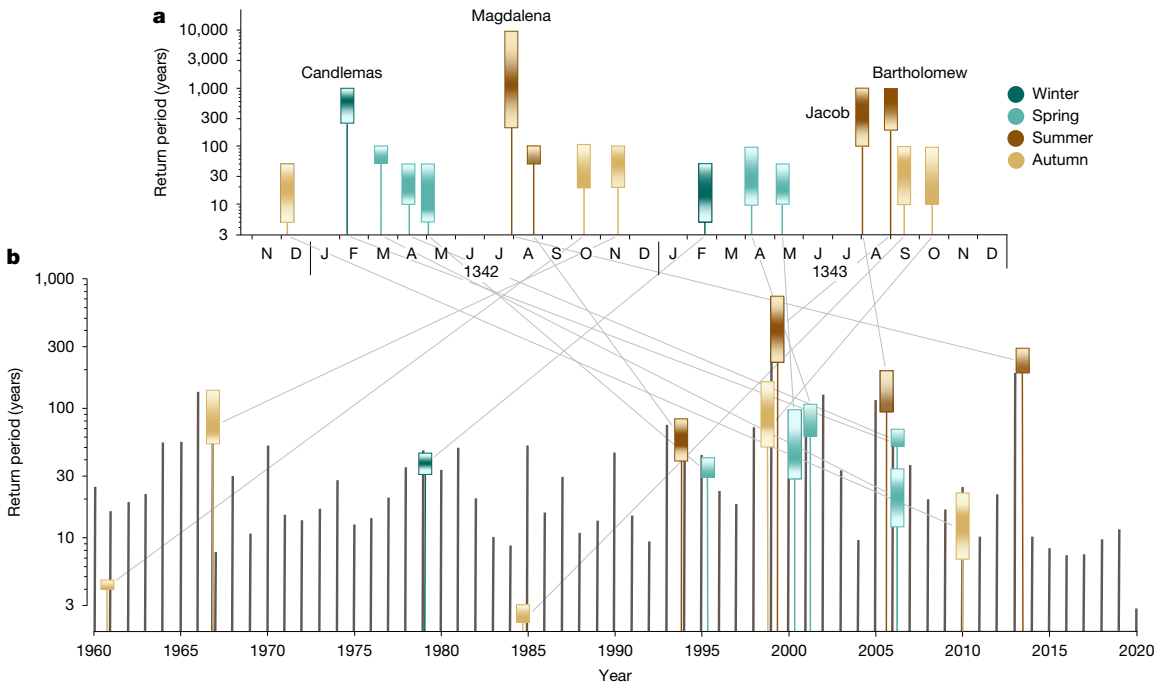

Fig. 5 | Closest-match analogues in the last six decades to the 16 European floods in 1341–1343. a, The largest known return periods of the 16 events in 1342–1343. Coloured boxes indicate the uncertainty ranges of the estimates with darker colours representing the most probable return periods. Letters on the x axis represent months of the year. **b**, Coloured boxes show the analogue events in 1960–2020 from Extended Data Tables 1 and 2 in terms of the 25%, 50% and 75% quantiles of the ten largest return periods in the flooded area[1]. Grey bars show the medians of the ten largest events at all locations of the analogue events; colours indicate the season of the floods.

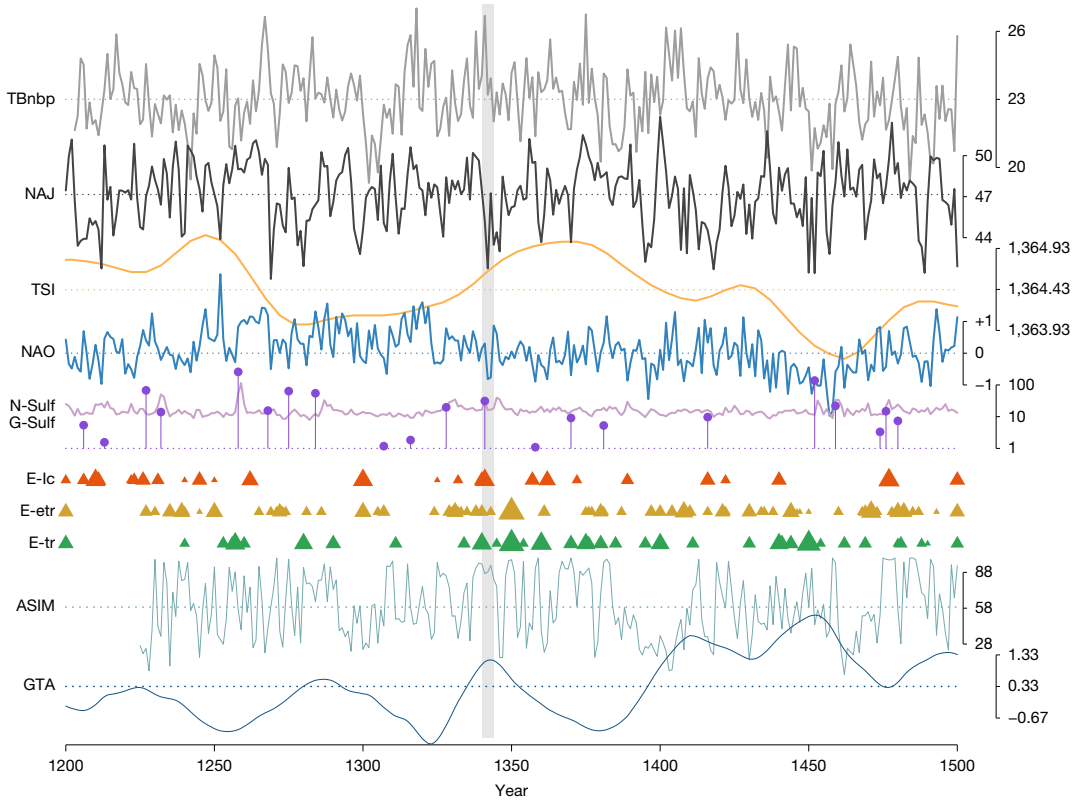

Fig. 6 | Possible extra- and intra-terrestrial causes of European extreme weather and floods. The graph shows possible causes of European extreme weather and floods. Coloured triangles, number of volcanic eruptions (size of triangles indicates the number of known eruptions per year from one to seven). ASIM, ratio of melted Arctic sea ice in summer (Franz Josef Land); E-Ic, Icelandic eruptions; E-etr, extratropical eruptions except Icelandic; E-tr, tropical eruptions; G-Sulf, global sulfate injection; GTA, Greenland annual temperature anomaly (normalized data; Supplementary Data 6); NAJ position, North Atlantic Jet Stream position; N-Sulf, Northern Hemisphere sulfate injection; TBnbp, tropical belt northern boundary position (indicator of the north boundary position of the Hadley cell); TSI, total solar irradiance. Grey bar, period 1340–1344. The unusual flood sequence can be explained by volcanic eruptions and Arctic sea ice decrease. For details on the variables, see Methods.

in Iceland (E-etr, E-Ic in Fig. 6). The Icelandic eruptions include the May–June 1341 explosive eruption of the Hekla (VEI = 3 (ref. 25) or 4 (ref. 26)), which induced mass livestock losses, land degradation, dearth and an important long-term migration in South-Iceland, supported by four reliable, local contemporary sources (for example. the Skálholt annals; Supplementary Information section 5.1). An extratropical eruption, probably the Hekla event, is also evidenced by atmospheric aerosol injections derived from ice-core deposition data[20] (N-Sulf in Fig. 6).

Although modest in terms of global aerosol forcing[20], recent observations and modelling studies indicate that, per unit sulfur injected into the stratosphere, extratropical eruptions of this size have a disproportionately large atmospheric impact[24,27], and can generate a Northern Hemisphere climate response around 7.5 times stronger than tropical eruptions, potentially exceeding the atmospheric impact of the 1991 Pinatubo eruption[28], especially if the eruption occurs in June[29].

Observations and climate simulations suggest that aerosol-induced stratospheric warming, caused by volcanic eruptions, combined with reduced incoming solar radiation tends to lead to Northern Hemisphere near-surface air cooling[30,31]. This cooling has probably induced the southward shift of the Intertropical convergence zone and the northern boundary of the Hadley cell from 1341 to 1342 (the tropical belt northern boundary position moved from 27° to 23°; Fig. 6) and moved the North Atlantic Jet Stream to a very southern position of 42° by 1342[32,33] (Fig. 6). Climate scenario simulations and reconstructions (Supplementary Information section 5.2; Methods) support a weakening effect of these processes on the polar vortex and polar jet, resulting in enhanced Rossby-wave meandering, a shift of the Arctic Oscillation and North Atlantic Oscillation (NAO) from positive to negative phases (NAO drops from +0.3 to −0.8 in Fig. 6), and a transition of El Niño–Southern Oscillation (ENSO) to a positive (El Niño) state in 1342[27,34,35]. Together, these circulation anomalies support an increased likelihood of high-intensity cyclones, prolonged rainfall and thus high-intensity flooding[27,36] (Supplementary Information section 5.2).

Another plausible contributing factor to the unusual sequence of floods is multi-annual Arctic warming (GTA in Fig. 6) and the decline in Arctic sea ice (ASIM in Fig. 6) from the mid-1330s onward (Supplementary Data 5 and Supplementary Information section 5.2). Reduced sea ice lowers surface albedo and increases North Atlantic sea surface temperatures[37]. The warmer sea surface conditions in the early 1340s[38], combined with lower near-surface temperatures related to volcanic activity, probably favoured more frequent and intense cyclones and increased mid-latitude European precipitation in the winters and summers of 1342–1343[37,39]. Arctic sea ice decline may also have contributed to the shift of the northern boundary of the Hadley cell between 1341 and 1342 (TBnbp in Fig. 6), and to a strong positive summer NAO[40,41], in combination with global climate modes[39] (Supplementary Information section 5.2; Methods). In addition, reduced sea ice probably amplified the eruption-induced shift of the Arctic Oscillation toward a negative phase and weakened the polar vortex, facilitating cold-air intrusions into Europe and enhancing rainfall in both winter and summer[40,41] (Supplementary Information section 5.2). Together, volcanic forcing, Arctic sea ice decline and their interaction represent plausible contributors to the exceptional flood sequence, alongside internal climate variability.

Why the other floods were forgotten

Although most of the literature[3,6,7,12] acknowledged only a single large-scale event in the period 1342 to 1343, known as the Magdalena Flood, the new dataset provides evidence of numerous major floods. Previous focus on a single event is due partly to the low temporal resolution of soil erosion and sedimentary evidence (Supplementary Data 2b). It also reflects the fragmentary survival of medieval documentary sources and the uneven geographical distribution of archives, which tend to privilege politically and economically central regions where no major destruction of medieval documents occurred later[16,42].

It is also surprising that, out of the 16 events described here, only the Magdalena Flood survived in public memory. This may be because it was the first time in the German areas when numerous flood marks and memorial plaques were mounted by local authorities and as a community effort and warning on the walls of iconic buildings[12] whereas, for example, no flood marks were set for the Candlemas Flood in Prague[43]. The establishment of such material markers has been shown to play a crucial role in shaping long-term risk awareness and collective memory[7,12,43]. Moreover, narrative amplification in chronicles and other documents may have reinforced the prominence of a single catastrophic episode, whereas closely spaced subsequent floods were perceived as continuations rather than distinct disasters. Institutional responses often crystallize around emblematic events, further marginalizing others in historiography[12,44].

Global extremes and future perspectives

The unusual flood years of the early 1340s in Europe align with extreme hydro-climatological conditions in other continents, suggesting a possible link through teleconnections (Supplementary Information section 5). Multi-annual Barents Sea ice retreat was aligned with extreme summer precipitation in Eastern Mongolia and Northeast China during 1342–1344, as well as with severe flooding of the Yangtze River, resulting in widespread dyke breaches and major disruptions to the Grand Canal, China's most important waterway[45,46]. On the other hand, precipitation on the Tibetan Plateau and streamflow of the Yellow River further in the south and of the Brahmaputra were very low[47,48], because of Monsoon failure—a typical response after major extratropical volcanic eruptions and Arctic sea ice decrease[43] (Supplementary Information section 5). Similarly, the 1341 to 1344 droughts in Yucatan, Guatemala[49] and New Mexico have been linked with volcanic eruptions and Arctic sea ice decrease[50]. In contrast, the White River in Arkansas shifted from extreme flooding in 1341 to very low flows in 1342, reflecting pronounced hydroclimatic variability in the south-central United States[51].

Current flood management decisions are based routinely on observations from recent decades and occasionally incorporate isolated historical floods. This study shows that sequences of very large floods, more extreme than those in recent decades, are possible and may occur again. Furthermore, climate projections suggest an increase of extreme extratropical cyclones in Europe[52] and observations point to increases in high-intensity convective events[53]. Megafloods that may affect the same, extensive areas within a few months have important implications for flood risk management. This is because current response of societies to extraordinary floods is usually slow, and it may take decades for flood mitigation measures to be implemented for political, financial and administrative reasons[54]. Current flood management is thus not necessarily prepared for such sequences. The results of this study suggest strongly that these implementation processes should be accelerated, and proactive flood risk management strategies that explicitly account for unusual sequences of extreme flood events are urgently needed, for example through adaptive planning approaches that consider cumulative impacts, flexible response capacities and local flood-proofing measures.

Online content

Any methods, additional references, Nature Portfolio reporting summaries, source data, extended data, supplementary information, acknowledgements, peer review information; details of author contributions and competing interests; and statements of data and code availability are available at https://doi.org/10.1038/s41586-026-10888-8.

1. Bertola, M. et al. Megafloods in Europe can be anticipated from observations in hydrologically similar catchments. *Nat. Geosci.* **16**, 982–988 (2023).
2. Blöschl, G. et al. Changing climate both increases and decreases European river floods. *Nature* **573**, 108–111 (2019).
3. Dreibrodt, S. & Bork, H.-R. In *Treatise on Geomorphology* 2nd edn. (ed. Schroder, J. F.) 547–560 (Elsevier, 2022).
4. Tetzlaw, G., Börngen, M., Mudelsee, M. & Armin, R. Das Jahrtausenhochwasser von 1342 am Main aus meteorologisch-hydrologischer Sicht. *Wasser u. Boden* **54**, 41–49 (2002).
5. Hofstätter, M. & Blöschl, G. Vb cyclones synchronized with the Arctic-/North Atlantic Oscillation. *J. Geophys. Res. Atmos.* **124**, 3259–3278 (2019).
6. Herget, J. et al. The millennium flood of July 1342 revisited. *Catena* **130**, 82–94 (2015).
7. Bauch, M. Die Magdalenenflut 1342 am Schnittpunkt von Umwelt- und Infrastrukturgeschichte. *NTM* **27**, 273–309 (2019).
8. Merz, B. et al. Understanding heavy tails of flood peak distribution. *Water Resour. Res.* **58**, e2021WR030506 (2022).
9. Brázdil, R. & Kotyza, O. *History of Weather and Climate in the Czech Lands I. Period 1000-1500* (ETH Zürich, 1995).
10. Kiss, A. Floods and weather in 1342 and 1343 in the Carpathian Basin. *J. Environ. Geogr.* **2**, 37–47 (2009).
11. Blöschl, G. et al. Current European flood-rich period exceptional compared with past 500 years. *Nature* **583**, 560–566 (2020).
12. Rohr, C. *Extreme Naturereignisse im Ostalpenraum. Naturerfahrung im Spätmittelalter und am Beginn der Neuzeit* (Vienna Böhlau, 2007).
13. Labbé, T. In *The Dance of Death in Late Medieval and Renaissance Europe. Environmental stress, Mortality and Social Response* (eds Kiss, A. & Pribyl, K.) 198–213 (Routledge, 2020).
14. Campbell, B. *The Great Transition. Climate, Disease and Society in the Late-Medieval World* (Cambridge Univ. Press, 2016).
15. Hunt, E. S. A new look at the dealings of the Bardi and Peruzzi with Edward III. *J. Econ. Hist.* **50**, 149–162 (1990).
16. Kiss, A. *Floods and Long-Term Water-Level Changes in Medieval Hungary* (Springer, 2019).
17. Lee, J., Perera, D., Glickman, T. & Taing, L. Water-related disasters and their health impacts: a global review. *Prog. Disaster Sci.* **8**, 100123 (2020).
18. Ionita, M., Nagavciuc, V. & Guan, B. Rivers in the sky, flooding on the ground: the role of atmospheric rivers in inland flooding in central Europe. *Hydrol. Earth Syst. Sci.* **24**, 5125–5147 (2020).
19. Wilson, R. et al. Last millennium northern hemisphere summer temperatures from the tree rings: Part I: the long term context. *Quat. Sci. Rev.* **134**, 1–18 (2016).
20. Sigl, M. et al. Timing and climate forcing of volcanic eruptions for the past 2,500 years. *Nature* **523**, 543–549 (2015).
21. *Global Volcanism Program – Volcanoes of the World 5.1.5* (Smithsonian Institution Global Volcanism Program, accessed 22 November 2025); https://volcano.si.edu/volcanolist_holocene.cfm.
22. Gao, C., Robock, A. & Ammann, C. Volcanic forcing of climate over the past 1500 years: an improved ice core-based index for climate models. *J. Geophys. Res. Atmos.* **113**, D23 (2008).
23. Toohey, M. & Sigl, M. Volcanic stratospheric sulphur injections and aerosol optical depth from 500 BCE to 1900 CE. *Earth Syst. Sci. Data* **9**, 809–831 (2017).
24. Toohey, M. et al. Disproportionately strong climate forcing from extratropical explosive volcanic eruptions. *Nat. Geosci.* **12**, 100–107 (2019).
25. Þórarinsson, S. *The Eruptions of Hekla in Historical Times: A Tephrochronological Study* (Leiftur, 1967).
26. Opała-Owczarek, M. et al. Slow growing juniper shrubs from northern Iceland record summer temperature changes over the last 800 years. *Quat. Sci. Rev.* **363**, 109441 (2025).
27. Sjolte, J., Adolphi, F., Guðlaugsdòttir, H. & Muscheler, R. Major differences in regional climate impact between highland low latitude volcanic eruptions. *Geophys. Res. Lett.* **48**, e2020GL092017 (2021).
28. Burke, A. et al. High sensitivity of summer temperatures to stratospheric sulfur loading from volcanoes in the Northern Hemisphere. *Proc. Natl Acad. Sci. USA* **120**, e2221810120 (2023).
29. Krawitz, B. & Robock, A. Climate effects of high-latitude volcanic eruptions: role of the time of year. *J. Geophys. Res.* **116**, D01105 (2011).
30. Paik, S. et al. Impact of volcanic eruptions on extratropical atmospheric circulations: review, revisit and future directions. *Environ. Res. Lett.* **18**, 063003 (2023).
31. Fuglestvedt, H. F., Zhuo, Z. & Krüger, K. Volcanic forcing of high-latitude Northern Hemisphere eruptions. *npj Clim. Atmos. Sci.* **7**, 10 (2024).
32. Osman, M. et al. North Atlantic jet stream projections in the context of the past 1,250 years. *Proc. Natl Acad. Sci. USA* **118**, e2104105118 (2021).
33. Zhuo, Z., Kirchner, I., Pfahl, S. & Cubasch, U. Climate impact of volcanic eruptions: the sensitivity to eruption season and latitude in MPI-ESM ensemble experiments. *Atmos. Chem. Phys.* **21**, 13425–13442 (2021).
34. Tao, Q., Shen, C., Muscheler, R. & Sjolte, J. Distinct winter North Atlantic climate responses to tropical and extratropical eruptions over the last millennium in PMIP simulations and reconstructions. *Clim. Past* **21**, 2561–2578 (2025).

35. Predybaylo, Y., Stenchikov, G., Wittenberg, A. T. & Osipov, S. El Niño/Southern Oscillation response to low-latitude volcanic eruptions depends on ocean pre-conditions and eruption timing. *Commun. Earth Environ.* **1**, 12 (2020).
36. Andreasen, L. S. et al. Changes in Northern Hemisphere extra-tropical cyclone frequency following volcanic eruptions. *Environ. Res. Clim.* **3**, 025002 (2024).
37. Ogawa, F. & Spengler, T. Influence of mid-latitude sea surface temperature fronts on the atmospheric water cycle and storm track activity. *Weather Clim. Dynam.* **5**, 1031–1042 (2024).
38. Cunningham, L. et al. Reconstructions of surface ocean conditions from the northeast Atlantic and Nordic seas during the last millennium. *Holocene* **23**, 921–935 (2013).
39. Chemke, R., Polvani, L. M. & Deser, C. The effect of Arctic sea ice loss on the Hadley circulation. *Geophys. Res. Lett.* **46**, 963–972 (2019).
40. Folland, C. K. et al. The Summer North Atlantic Oscillation, Arctic sea ice, and Arctic jet Rossby wave forcing. *Sci. Adv.* **10**, eadk6693 (2024).
41. Cohen, J., Francis, A. J. & Pfeiffer, K. Anomalous Arctic warming linked with severe winter weather in Northern Hemisphere continents. *Commun. Earth Environ.* **5**, 557 (2024).
42. Pfister, C. Klimawandel in der Geschichte Europas. Zur Entwicklung und zum Potenzial der historischen Klimatologie. *Österr. Z. Gesch.-wiss.* **12**, 7–43 (2001).
43. Fanta, V., Šálek, M. & Sklenicka, P. How long do floods throughout the millennium remain in the collective memory? *Nat. Commun.* **10**, 1105 (2019).
44. Lübken, U. *Die Natur der Gefahr: Überschwemmungen am Ohio River im 19. und 20. Jahrhundert* (Vandenhoeck & Ruprecht, 2014).
45. Li, T. in *The Crisis of the 14th Century. Teleconnections between Environmental and Societal Change?* (eds Bauch, M. & Schenk, G.) 100–129 (DeGruyter, 2020).
46. Cook, E. R. et al. Asian monsoon failure and megadrought during the last millennium. *Science* **328**, 486–489 (2010).
47. Yang, B. et al. A 3,500-year tree-ring record of annual precipitation on the northeastern Tibetan Plateau. *Proc. Natl Acad. Sci. USA* **111**, 2903–2908 (2014).
48. Rao, M. P. et al. Brahmaputra River 700 year monsoon season streamflow reconstruction. *Nat. Commun.* **11**, 6017 (2020).
49. Cook, E. R. et al. Megadroughts in North America: placing IPCC projections of hydroclimatic change in a long-term palaeoclimate context. *J. Quat. Sci.* **25**, 48–61 (2010).
50. Meko, D. M. et al. Medieval drought in the upper Colorado River Basin. *Geophys. Res. Lett.* **34**, L10705 (2007).
51. Cleaveland, M. A 963-year reconstruction of summer (JJA) streamflow in the White River, Arkansas, USA, from tree-rings. *Holocene* **10**, 33–41 (2000).
52. Priestley, M. D. & Catto, J. L. Future changes in the extratropical storm tracks and cyclone intensity, wind speed, and structure. *Weather Clim. Dynam.* **3**, 337–360 (2022).
53. Haslinger, K. et al. Increasing hourly heavy rainfall in Austria reflected in flood changes. *Nature* **639**, 667–672 (2025).
54. Kreibich, H. et al. The challenge of unprecedented floods and droughts in risk management. *Nature* **608**, 80–86 (2022).

Publisher's note Springer Nature remains neutral with regard to jurisdictional claims in published maps and institutional affiliations.

Open Access This article is licensed under a Creative Commons Attribution 4.0 International License, which permits use, sharing, adaptation, distribution and reproduction in any medium or format, as long as you give appropriate credit to the original author(s) and the source, provide a link to the Creative Commons licence, and indicate if changes were made. The images or other third party material in this article are included in the article's Creative Commons licence, unless indicated otherwise in a credit line to the material. If material is not included in the article's Creative Commons licence and your intended use is not permitted by statutory regulation or exceeds the permitted use, you will need to obtain permission directly from the copyright holder. To view a copy of this licence, visit http://creativecommons.org/licenses/by/4.0/.

© The Author(s) 2026

Methods

Development of the historical flood database

Flood evidence in Europe over the period 1341–1343 was collected from narrative sources (chronicles, annals) and legal and economic administrative documentation (charters, accounts) as well as other documentary source types (thanksgiving inscriptions/memorials, scientific discussion, flood marks) (Supplementary Data 1–3). Although chronicles provided most of the information in most parts of Europe, in some areas, such as the Carpathian Basin, charters were more relevant[16]. Chronicles and annals often captured the greatest floods in a systematic way, but did not cover smaller floods or floods that occurred shortly after a great one. The other source types provided non-systematic evidence on individual flood events and were usually more precise in location.

We applied critical historical source evaluation, removing evidence deemed unreliable, and separating contemporary and non-contemporary sources: around 77% of the flood data entries come from contemporary sources, the rest from medieval sources based on earlier, contemporary source evidence. All floods are covered by contemporary sources, and other medieval sources were only used as complementary evidence. For over 70% of the floods, several types of independent contemporary source evidence was available. Giving priority to contemporary sources sets this study apart from previous research and enhances its reliability, as contemporary sources are first-hand information. This process resulted in 168 flood entries in the database on 60 European rivers, and four large lakes and wetlands.

In the period 1341–1343, several major floods occurred on the same river, including the Rhine, Tisza, Po, Elbe, Danube, Axios, Main, Inn, Drava and the Altmühl. For example, in the upper sections of the Tisza River, three major and two notable independent floods were recorded. Inspired by the term 'Magdalena Flood' used to describe the flood that peaked on the day of Saint Maria Magdalena, we propose similar names for three other major floods: the Candlemas, Jacob and Bartholomew Floods (Extended Data Tables 1 and 2).

Magnitude class and return period estimation

We assess the magnitudes of each event in two ways. In a first step, we categorize each flood during 1341–1343 into one of three classes, consistent with the 500-year European database[11] using the source texts, where class 1 represents notable floods, class 2 great floods and class 3 extraordinary floods. As more detailed information was available for the 1341–1343 floods than for the 500-year series, we also assign return periods in a second step. As expert-based, interpretative assessments, the return periods (Fig. 5) draw on a comprehensive collation of local and regional historical quantitative and qualitative water-level data, complemented by archaeological and sedimentary evidence. Even where quantitative indicators such as preserved flood marks are available, their interpretation necessarily reflects the substantial long-term modification of catchments and river systems. Accordingly, the estimates should be understood as contextually informed reconstructions that integrate several lines of evidence within an evolving environmental framework. Direct comparisons between medieval and modern floods are complicated by substantial anthropogenic changes in river morphology, floodplains and catchment hydrology since 1342. Accordingly, our return period estimates do not rely on direct comparisons of absolute flood levels or damage with modern gauged floods, but instead use a relative, rank-based approach that is standard practice in historical flood hydrology. We both identify most likely return periods and an uncertainty range. The method, detailed in Supplementary Information section 1, depends on the information available[55]:

1. Exact numerical information on the maximum water level or the maximum flood extent: these cases were compared with modern floods where the relationship between water level and return period are known, taking into consideration the possible uncertainties and changes that occurred in the landscape, hydromorphology, hydrology and river dynamics over time. Most of the maximum water-level estimations presented in Fig. 5 belong to this category. For example, based on flood marks and maximum water-level descriptions with exact localization, with additional information about changes in the environmental conditions such as the landscape, the town wall and the river morphology, the Magdalena Flood on the Main at Würzburg was estimated as a 1,000-year return period flood, and uncertainty ranges were identified[6]. Based on the report by local monk Johann von Winterthur[56] that the Barfüsser Church was flooded up to the upper church (or podium), and on the account by Heinrich von Diessenhofen that, at roughly the same time, the town wall of Konstanz was overtopped only at the Dominican Friary, we estimated the return period of the Bartholomew flood in Lindau to be around 1,000 years[57–60] (Supplementary Information section 1). This estimate accounts for lake sedimentation rates, differences in church floor elevations in Lindau and the known height of the medieval town wall in Konstanz Return period estimate with uncertainties for the same flood are also available for the Upper Rhine at Basel[55,60] (Supplementary Information section 1). Contemporary chronicler Fritsche Closener[58] wrote that the Bartholomew Flood was 2 feet higher than the Jacob Flood in Strasbourg, from which the differences in the return periods on the Rhine were estimated. Contemporary sources also report the height of water standing in churches (for example, in Vendôme and Luzern) and note that churches in Rouen and Luzern could be entered by large boat during the Candlemas and Jacob Floods, respectively. From these accounts water levels and return periods were inferred, considering elevation changes. In many cases hydro-morphological, and archaeological data were used to assist in the comparison between fourteenth century and modern conditions (Supplementary Information section 1).
2. Descriptive, quasi-numerical information related to the flood magnitude. In this case, the return period was inferred from the assessed frequency of how often a similar situation occurred over the centuries and how unusual it was in terms of infrastructure damage. For instance, during the Candlemas Flood in Prague[59], where two-thirds of the famous Judith stone bridge were destroyed, we estimated a return period of at least 300 years. This estimate is based on the fact that the bridge was constructed in the twelfth century, taking previous floods into consideration. The Candlemas Flood was probably the most outstanding flood in several hundred years.

   The exceptionally severe damage to riverine infrastructure and town buildings, together with mass fatalities and the destruction of entire villages, supports this estimate (Franciscus Pragensis)[59]. Based on this and other information, such as a late medieval flood mark, and alluviation data from archaeological profiles, the return period of Candlemas in Prague was estimated as 500 years with a lower limit of the uncertainty range of 300 years. The upper limit of the uncertainty range was estimated as 1,000 years from the fact that the Roudnice bridge 50 km downstream of Prague was not damaged (Supplementary Information section 1). These estimates are similar to the Candlemas return periods for Vendôme estimated in step 1.

   Similarly, Heinrich von Diessenhofen[60] reported that during the Jacob Flood all bridges along the Rhine between Schaffhausen and Strasbourg were completely destroyed and Johann von Winterthur[56] noted that the vineyards (never placed in flood-prone areas) and entire districts of Lindau were destroyed, suggesting a return period of around or greater than 100 years (Supplementary Information section 1).
3. Information on the flood magnitude expressed by the choice of language and the broader environmental, legal or military implications: Here again, the return period was inferred from the assessed frequency of the event and, in some cases, from infrastructure damage, which provided indications of how far flood waters extended

across the landscape and thus allowed estimation of water levels. The mid-March 1342 flood[61] at the lower sections of the Upper Tisza obstructed the legal processes over debated land boundaries to the extent that survey participants could not even reach the region of the settlements in question, suggesting an event that does not happen more often than once or twice a century[16]. In the same area the medieval environment was described in this and other charters with exact dating, and detailed maps are also available in the eighteenth and nineteenth centuries, which make it possible to locate the flood and its approximate extension[16].

The Strassburger Chronik of Fritsche Closener[58] describes the Jacob Flood at the Rhine "Do man zalte 1343 jor, do wart (der) Rin also groß und ging also sere us, daz nieman do zemol lebete der üt gedohte oder ie hette gehoret sagen, daz er so groß würde." (The flood level and extent was beyond imagination of anybody living or any reports), from which we inferred a minimum 100-year return period (three generations), based on an interpretation of communicative memory[62]. More broadly, the term 'diluvium' (deluge) appears only rarely in medieval Latin texts and is generally understood to denote events with a return period of several hundred years, and therefore related to cultural memory[62]. It is used for all four major floods, for example, by Heinrich von Taube[63] for the Magdalena and Jacob floods in Eichstätt, and by Franciscus Pragensis for the Candlemas Flood in Prague[59].

Further details are available in Supplementary Information section 1, where case studies of return period estimations are presented on the examples of the Candlemas, Magdalena, Jacob and Bartholomew Floods, and are based on refs. 64–157.

Development of historical weather database

We have developed a European weather database for the 1341–1343 period (Supplementary Data 2a). It contains 213 entries, of which 98% are from contemporary sources and 2% stem from the late fourteenth century and fifteenth century (Extended Data Table 2). The sources include weather reports, providing daily, monthly and seasonal resolution, from chronicles, legal administrative sources (charters, official letters), manorial accounts and, occasionally, contemporary scientific discussions. To understand the continental-scale weather, we also use part of the contemporary weather diary of William Merle[158], which contains daily entries with monthly and seasonal summaries for Central and Southeast England during 1341–1343. About 20% of the weather data come from the same sources as the flood reports and identify explicitly the cause of flooding. They are listed in Supplementary Data 1a (column U). The remaining 80% of the weather data were reported in sources different from those of the floods, and provide corroborative information. They are shown in Fig. 2c,d and given in Supplementary Data 2a. We identify weather events including heavy precipitation, low temperature, high temperature, wind and hail/storms, and classify them into three classes, similar to the floods. We also identify the presence of atmospheric blocking, when prolonged clear skies, sunshine and extended periods of dry (and in summer hot) weather were reported. Two events were classified as Vb events[159] (Extended Data Table 2 and Supplementary Information section 1), which are associated with cyclones originating near the western Mediterranean or Gulf of Genoa and moving northeastward across northern Italy toward central/eastern Europe, turning counterclockwise. The classification was based on several characteristics known to be associated with Vb events[5], sometimes reported by eye witnesses, such as heavy rainfall in the Northern Alps, flooding in the Upper Danube basin and of Lake Constance, and a preceding shift to strong southwesterly winds in southern England (Supplementary Data 6a). Tree-ring based cloud cover[160], sea surface[38] and air temperature[19] reconstructions provide indirect information on atmospheric pressure, suggesting stationary summer high pressure systems over the North Sea and the Atlantic coastline of Northern Europe and thus blocking in 1342 and 1343.

The temporal coherence and wide spatial extent of the reports can be used to infer large-scale hydroclimatic conditions even where local weather data are missing. For example, although direct weather information is lacking for western France during the Candlemas Flood (event 2), contemporary sources (column AB in Supplementary Data 1) provide precise timing, duration and the causes of flooding on the Loir, Eure and Seine, which match closely flood reports from Germany, Czechia and Central Europe as far east as the Western Carpathians (rows 9–16 in Supplementary Data 1a), and are consistent with daily weather observations from southern England (Supplementary Data 2a).

Development of the historical impact database

A concise historical flood and extreme weather impact database was developed comprising 363 recorded impacts at more than 100 locations, 98% of which come from contemporary sources. Direct, immediate impacts include damage to infrastructure, agriculture, livestock and human life, as well as direct and immediate societal reactions. In 99% of cases, the contemporary sources attribute these impacts explicitly to flooding or extreme weather. In the remaining few cases, impacts are not attributed explicitly but are inferred from clear contextual indicators such as grain prices and salt production problems. These direct, immediate impacts are listed in Supplementary Data 3, with links to Extended Data Table 4, where impacts were classified into 28 categories and aggregated into six main impact groups. Original source texts on flood damages, and information on examples of associated prevention measures are given in Supplementary Information section 2, and are based on refs. 161–169.

Indirect, longer-term flood and extreme weather impacts, food shortage, grain prices, dearth, famines and associated socio-economic responses are discussed and interpreted in a broader, multi-annual European context in Supplementary Information section 3, and are based on refs. 170–207.

Comparison of the number of great floods per year with past 700 years

For placing the 1342–1343 period into a longer historical context, we extended the 103 documentary-based European flood series from 1500 to 2010[11] to the beginning of the fourteenth century (Fig. 4, Extended Data Fig. 2 and Supplementary Data 4), utilizing the published collection of great and outstanding medieval floods in Europe with an emphasis on Central Europe[16]. This database was further enhanced with the data based on a systematic check of the medieval historical data (using critical source analysis) available in the grand European collection of weather and weather-related hydrological phenomena[208]. We included in our database only the (major) flood events of more important flood years that could be traced and critically evaluated in the original historical source context. We also added 59 new flood series to increase the overlap with the rivers affected by the 1342–1343 floods, using principal data collections[209,210] and local sources[9,12,16,211], applying critical source evaluation and giving priority to contemporary source evidence. The new database used here thus contains 161 flood series from 1300 to 2010. Because of the enormous quantity of databases and original sources that had to be checked through and critically evaluated, regarding the additional flood data (added to the 500-year database) we focused on major flood years and the floods marked as great or outstanding (index 2 and 3) in magnitude. We applied the same bias correction to the new database as that applied to the original 1500 to 2010 database[11], which corrects for likely missed small or no-events in years without records.

Identification of modern analogue events

To gain a better understanding of the potential characteristics of the historical events, we identified modern analogues to the 1342–1343 flood events, similar to the facial reconstruction sometimes done in palaeontology (Extended Data Tables 1 and 2 and Supplementary

Information section 4). We selected the modern analogues based on the following similarity criteria: timing and seasonality, duration, causes and weather background, magnitude, location and minimum spatial extent. We scrutinized scientific publications, hydrological reports and relevant newspaper and online news entries related to damaging floods and their weather conditions in 1960–2020, and also use the European flood database of annual maximum discharge[1]. Given that much of the historical information is qualitative, the similarity criteria were applied manually by qualitative judgement. The comparison resulted in between three and five analogue events, ranked by their similarity, for each of the 16 historical events (Supplementary Information section 4). The top ranked events are presented in Extended Data Tables 1 and 2 and are shown in Fig. 5b. The modern analogues fill in the gaps where no historical information is available in 1342–1343, but they result in potential, reconstructed spatial distributions and durations (Supplementary Data 5).

The final reconstructed flood patterns are shown as ellipsoids in Fig. 1 and represent a conceptual depiction of the likely spatio-temporal extent of flooding, based on historical flood and meteorological evidence, complemented by modern analogues where the historical record is incomplete (Extended Data Fig. 1). The use of ellipsoids is a deliberate choice to balance overfitting and underfitting of the available historical data.

Each ellipsoid is based on the number, timing and spatial coherence of reported flood events (Supplementary Information section 4 and Extended Data Fig. 1). When only two or three contemporaneous floods were documented on different European rivers, we applied a multi-step validation procedure. We first consulted the pan-European flood database[1] to identify modern analogue events in which the same rivers flooded simultaneously or near-simultaneously, thereby assessing whether sparse historical reports could represent a larger-scale hydroclimatic event rather than isolated local extremes. Second, for each candidate analogue, we compared documentary weather information from before and during the 1342–1343 floods (Supplementary Data 2) with modern meteorological data from analogous flood events at both continental and regional scales. At the continental scale, we assessed reconstructed and observed European synoptic circulation patterns to evaluate whether the historical floods were associated with coherent large-scale atmospheric configurations (for example, persistent low-pressure systems or zonal flow anomalies). At the regional scale, we examined weather conditions within the affected river catchments, including precipitation persistence, temperature anomalies and antecedent soil-moisture conditions where available. These comparisons drew on pan-European reanalysis products, national daily and monthly weather records, and publicly accessible archives such as NOAA and Climate Explorer. A full description of the comparison between historical flood, weather and the modern analogues, and the coverage of the flood is given in Supplementary Data 5 and Supplementary Information section 4, and are based on refs. 212–333.

The agreement between the spatial structure of modern analogue floods, associated atmospheric circulation patterns, and fourteenth century documentary evidence informed the size, orientation and placement of each ellipsoid, ensuring that the reconstructed flood patterns reflect both the historical reports and their physical plausibility within a continental-scale hydroclimatic framework.

Attribution of the 1341–1343 floods

To shed light on the physical reasons for the unusual 1342–1343 flooding (Fig. 6), data were obtained from the following sources (Supplementary Data 5). The tropical belt northern boundary position—an indicator of the north boundary position of the Hadley cell—is based on spring-precipitation reconstruction from tree-ring evidence of five mid-latitude regions[334]. The North Atlantic Jet Stream position is derived from an ensemble of water-isotope based climate model simulations, and the mean annual water isotope ($\delta^{18}O$) and annually accumulated snowfall records detected in Greenland ice cores[32]. The total solar irradiance is based on paleoclimate (temperature, coral $\delta^{18}O$) proxies and model simulation[335].

The annual index values of the NAO in the last millennium, applied in this study, were reconstructed based on 48 proxy series derived from ice cores, lake sediments, speleothems or tree rings[336]. Global and Northern Hemisphere sulfate injection series were initiated from the sulfate deposition content in Arctic, Greenland and Antarctic ice cores[337]. Arctic annual (normalized) temperature data in Greenland and summer sea ice melting data in Franz Josef Land in the Barents Sea, were derived from ^{18}O ratio in ice cores[338,339]. Possible causative atmospheric links and process mechanisms from experimental case studies and climate simulations are discussed in Supplementary Data and Supplementary Information section 5.

Data on the number of volcanic eruptions are derived from the Smithsonian Institution GVP database[21], and were divided into Icelandic eruptions (E-Ic), northern hemispheric extratropical eruptions excluding Icelandic (E-etr) and tropical eruptions (E-tr). The VEI, representing the magnitude and intensity of eruptions, is based on the Smithsonian Institution GVP database[21] including its references that use a range of information such as lake sediments, ice cores and documentary evidence (Supplementary Data 6). This database includes small and large eruptions, whereas key publications and related databases[20,337,340] discuss only the largest eruptions. The atmospheric impact of eruptions through volcanic radiative forcing and sulfate injection has been evidenced in the literature[20,22–24,27–31].

Historical archives clearly document eruptions of Hekla and probably also other Icelandic volcanoes, such as the Eyjafjallajökull, around 1341 (Supplementary Information section 5). However, it remains difficult to assess whether these eruptions injected material into the stratosphere or whether aerosols were mostly tropospheric with limited impacts on climate. The 2010 Eyjafjallajökull eruption provides a useful modern analogue. One way to further test the proposed hypothesis would be to investigate sulfur isotope ($\Delta^{33}S$) measurements in ice-core records for the 1341 event, to discriminate between stratospheric and tropospheric sulfate deposition[28,341].

Although the climate response and the floods of winter 1341–1342 show strong similarities to those of winter 1783–1784 following the Laki eruption[342], an important difference is the decrease in Arctic sea ice in the late 1330s to early 1340s, which was absent in the early 1780s and which may also have contributed, among other factors, to the considerably wetter-than-usual summers of 1342 and 1343.

To further strengthen the interpretation, it may be worthwhile to conduct specific climate simulations using current aerosol optical depth reconstructions for the 1341 event[340,343,344] to assess the likelihood of enhanced precipitation or flood-favourable circulation patterns. In addition, it would be useful to examine existing paleo-reanalyses, such as the Global 2000-Year Paleo Hydrodynamics Data Assimilation product[343], which provide estimates of large-scale modes of variability.

Causative data, climate comparisons and global climate indices in 1341–1343 are available in Supplementary Information section 5, and are based on refs. 345–395.

Estimation of Arctic Oscillation and NAO

NAO reconstructions[336,396–398] sometimes show significant discrepancies, leading to a somewhat conflicting view of annual and winter NAO. Furthermore, there are no summer NAO reconstructions that extend back to the 1340s[399]. Thus, we analysed the documentary and natural proxy data of the seasonal and annual weather in 1342 and 1343 (Supplementary Data 2a,b), using the NAO–weather relationship presented by the United Kingdom Met Office[400], to identify the seasonal signs of the NAO. The severe cold outbreaks in mid-latitudes and the unusually high temperatures observed in some high-latitude areas[401–403] suggest prevailing negative winter Arctic Oscillation and NAO values in 1342

and 1343, which is consistent with a previous annual reconstruction[336]. Comparisons with contemporary data and modern simulations indicate that summer patterns probably exhibited prevailing positive NAO mode during both years because of the anomalously wet and cool conditions in the Mediterranean and the prevailing dry and warm patterns in the North Atlantic (Supplementary Data 2a,b).

For linking European weather in 1341–1343 to global climate processes, we also examined reconstructions of other Northern, Southern Hemispheric and global climate mode indices. For example, the combination of negative Arctic Oscillation and NAO, presence of the East Atlantic pattern and positive ENSO along with a positive Indian Ocean Dipole could be important contributing factors to the unusually severe and wet winter in 1342 (Supplementary Information section 5.2).

Data availability

All flood- and weather-related documentary source data are available as Supplementary data.

Code availability

No code was used in the data analysis.

55. Salinas, J., Kiss, A., Viglione, A., Viertl, R. & Blöschl, G. A fuzzy Bayesian approach to flood frequency estimation with imprecise historical information. *Water Resour. Res.* **52**, 6730–6750 (2016).
56. Baethgen, F. *Monumenta Germaniae Historica. Scriptores rerum Germanicarum, Nova Series*, Vol. 3. *Die Chronik Johanns von Winterthur* (Weidmannsche Buchhandlung, 1924).
57. Strobel, A. W. & Schott, A. In *Bibliothek des Literarischen Vereins in Stuttgart* (ed. Strobel, A. W.) 1–127 (Literarischer Verein, 1842).
58. Loserth, J. *Fontes Rerum Austriacarum. Oesterreichische Geschichts-Quellen. Königsaaler Geschichts-Quellen / Domherr Franz von Prag. Vol. 1: Scriptores*, Vol. 8 (Gerold, 1875).
59. Böhmer, J. F. *Fontes rerum Germanicarum. Geschichtsquellen Deutschlands*, Band 4: *Heinricus de Diessenhofen und andere Geschichtsquellen Deutschlands im späteren Mittelalter* (Cotta, 1868).
60. Hungarian National Archives, Archival Documents of Medieval Hungary. 31242: *Charter of the Chapter of Eger*, issued 24 May 1342.
61. Wetter, O. et al. The largest floods in the High Rhine basin since 1268 assessed from documentary and instrumental evidence. *Hydrolog. Sci. J.* **56**, 733–758 (2011).
62. Assmann, J. in *The Theoretical Foundations of Hungarian 'Lieux de Mémoire' Studies. Loci Memoriae Hungaricae 1* (eds Varga, P. S. et al.) 36–43 (Debrecen Univ. Press, 2013).
63. Bresslau, H. *Scriptores rerum Germanicarum, Nova series 1: Die Chronik Heinrichs Taube von Selbach* (Weidmann, 1922).
64. Braun, G. *Civitates Orbis Terrarum*. *Liber Quartus* (1588).
65. Brázdil, R. & Dobrovolný, P. Floods in the Czech Republic during the past millennium. *Houill. Blanche* **5**, 50–55 (2004).
66. Tyraček, J., Westaway, R. & Bridgland, D. River terraces of the Vltava and Labe (Elbe) system, Czech Republic, and their implications for the uplift history of the Bohemian Massif. *Proc. Geol. Assoc.* **115**, 101–124 (2004).
67. Čiháková, J. Fortification of the southern and eastern perimeter of the early Gothic predecessor of today's Malá Strana. *Staletá Praha* **38**, 86–157 (2022).
68. Havrda, J. & Tryml, M. Medieval pavements in the old town of Prague. An archaeological contribution to the knowledge of the history of communications. *Staletá Praha* **25**, 41–52 (2009).
69. Elleder, L., Herget, J., Roggenkamp, T. & Nießen, A. Historic floods in the city of Prague—reconstruction of peak discharges. *Hydrol. Res.* **44**, 202–214 (2013).
70. Kozáková, R. & Pokorný, P. Dynamics of the biotopes at the edge of a medieval town. *Preslia* **79**, 259–281 (2007).
71. Havrda, J. Archaeological evidence of floods in medieval and early modern Prague. In *Proc. 3rd PAGES Paleoflood Group Workshop* (PAGES, 2025).
72. Hrdlička, L. K proměnám středověké Prahy. In *Prague: A Hub of European Culture. International Symposium ICOMOS2000* (eds Kovaříková, L. et al.) 48–53 (ICOMOS, 2000).
73. Hrdlička, L. in *Neživá příroda Prahy a jejiho okolí* (eds Kovanda, J. et al.) 201–212 (ICOMOS Czech National Committee, 2001).
74. Kiss, A. & Laszlovszky, J. 14th-16th-century Danube floods and long-term water-level changes in archaeological and sedimentary evidence in the western and central Carpathian Basin: an overview with documentary comparison. *J. Environ. Geogr.* **6**, 1–11 (2013).
75. Kiss, A. & Laszlovszky, J. in *Islands, Monasteries and Water—Liquid Life on Liminal Land* (eds Hüglin, S. et al.) Ch. 13 (Sidestone, 2026).
76. Brázdil, R., Kotyza, O. & Dobrovolný, P. July 1432 and August 2002— two millennial floods in Bohemia?. *Hydrol. Sci. J.* **51**, 848–863 (2006).
77. Elleder, L. Historical changes in frequency of extreme floods in Prague. *Hydrol. Earth Syst. Sci.* **19**, 4307–4315 (2015).
78. Podliska, J. & Semerád, M. Nové poznatky o konstrukci Juditina mostu v Praze. *Staletá Praha* **28**, 121–136 (2012).
79. Havrda, J. in *Archeologický výzkum v Praze v letech 2011–2012* (eds Dragoun, Z. et al.) Pražský sborník historický 41, 489–490 (2013).
80. Podélný profil dolní Vltavy v Praze od ústí Berounky až k ústí Labe: Vodopis československé republiky, řada V, sešit 12, svazek 166, Státní ústav hydrologický T.G. Masaryka v Praze Podbabě https://www.lvvc.cz/databaze.php?UDALOST=33 (1951).
81. Cihla, M. & Panáček, M. in *Archäologie der Brücken/Archaeology of Bridges* (ed. Bayerische Gesellschaft für Unterwasserarchäologie & Bayerischen Landesamt für Denkmalplege) 240–246 (Pustet, 2011).
82. Kolářová, D. Two historical bridges in one in Roudnice nad Labem. *IOP Conf. Ser. Mater. Sci. Eng.* **1203**, 022014 (2021).
83. Herget, J. *Am Anfang war die Sintflut – Hochwasserkatastrophen in der Geschichte* (Wissenschaftliche Buchgesellschaft, 2012).
84. Richter, O. *Geschichte der Stadt Fresden. Erster Theil: Dresden im Mittelalter* (Baensch, 1900).
85. Bartl, S. et al. Zur Rekonstruktion langjähriger Wasserstands- und Durchflusszeitreihen am Elbepegel Dresden. *Hydrol. Wasserbewirtsch.* **52**, 162–167 (2008).
86. Municipal Library of Rouen. Chron. mscr. S. Katharinae, apud chron. triplex et unum, folio 162.
87. Braun, G., Hogenberg, F. & Novellanus, S. *Civitates Orbis Terrarum. Liber Primus* (Kempen, 1572).
88. Le Lieur, J. La Grande Vue de Rouen en 1525. Miniature centrale: Jacques Le Lieur remettant le Livre des Fontaines aux conseillers municipaux, dans une salle de 'l'Hostel-commun', le 30 janvier 1526. *Rotomagus* https://www.rotomagus.fr/ark:/12148/btv1b100500169. image (n.d.).
89. Gomboust, J. Plan de Rouen, réalisé par Gomboust en 1655. *Wikimedia* https://commons.wikimedia.org/wiki/File:Plan_assembl%C3%A9_Rouen_-_Gomboust_1655.jpg.
90. Richard, C. V. L. *Recherches historiques sur Rouen: fortifications, Porte Martinville* (Péron, 1844).
91. Le Cautan, M. La chapelle Notre-Dame-du-Parc, prieuré de Grandmont, à Rouen. *Bull. Monumental* **92**, 207–219 (1933).
92. Dion, R. Observations sur le site de la ville de Rouen. *Ann. Geogr.* **41**, 131–142 (1932).
93. Sadourny, A. Les transports sur la Seine aux XIIIe et XIVe siècles. *Ann. Bretagne Pays Ouest* **85**, 231–244 (1978) .
94. Frouin, M., Sebag, D., Durand, A. & Laignel, B. Palaeoenvironmental evolution of the Seine River estuary during the Holocene. *Quaternaire* **21**, 71–83 (2010).
95. Foussard, V. et al. *Évolutions Morphologique d'un Estuaire Anthropisé de 1800 à Nos Jours. Fascicule Seine-Aval, GIP Seine-Aval 2.3*. (Seine-Aval, 2010).
96. Sorrel, P. et al. Evidence for millennial-scale climatic events in the sedimentary infilling of a macrotidal estuarine system, the Seine estuary (NW France). *Quat. Sci. Rev.* **28**, 499–516 (2009).
97. *Rouen topographic map* (Topographicmap.com, accessed 11 December 2025); https://en-gb.topographic-map.com/map-l1pcz/Rouen/?center=49.4387%2C1.0996&zoom=17&popup=49.43986%2C1.09762.
98. Bordas-Demoulin, J.B. *Chorographie du Dunois ou Notice sur les Villes, Bourgs, Fiefs, Justices, Châteaux: Maisons de Campagne de Quelque Importance qui y Sont Renfermés* (ed. Achille Guenée, M.) 9–10 (Lecesne, 1851).
99. Souchet J.-B. *Histoire du Diocèse et de la Ville de Chartres*, Tome 3 (Garnier, 1869).
100. Chevard, V. *Histoire de Chartres et de l'Ancien Pays Chartrain: Avec une Description Statistique du Département d'Eure et Loir*, Tome 2 (Durand-le-Tellier, 1801).
101. Héliot, P. & Jouven, G. L'église Saint-Pierre de Chartres et l'architecture du Moyen Âge. *Bull. Archeol. Comit. Trav. Histor. Sci.* **6**, 117–177 (1970).
102. Borderie, Q. et al. Castles in townscapes: studying fortified medieval towns and their environments in Eure-et-Loir (France). *Landscapes* **20**, 139–159 (2021).
103. Braun, G. *Urbium praecipuarum totius mundi. Liber Tertius* (Cologne Brachel, [1581] 1616). Table 8; https://polona.pl/item-view/6d35677c-c571-47bf-b160-9791501eb614?page=1.
104. Boudan, L. Veue de l'Abbaye: De St Pere en Valee a Chartres. Gallica Digital Library, digital ID btv1b69018265 (1696).
105. *Global elevation and flood map* (Floodmap, accessed 23 February 2026); http://www.floodmap.net.
106. Annales Trinitatis Vindocinensis. in L. *Recueil d'annales angevines et vendômoises. Collection de Textes (pour servir a l' étude et a l'enseignement de l'histoire)* (ed. Halphen, L.) 50–79 (Picard, 1903).
107. Mesmin, E. et al. Characterization of periods of high and low hydrological activity in the Loire River, France, between the 14th and mid-19th centuries. *J. Hydrol.* **633**, 130932 (2024).
108. Piana, J. et al. Dynamique paysagère tardiglaciaire et holocène dans la vallée du Loir à Pezou (Loir-et-Cher): développements méthodologiques et premiers résultats. *Norois* **213**, 73–88 (2009).
109. Pasquier, J.-C. Le Loir en Vendômois. *B. Soc. Arch. Vend.* **51**, 149–160 (2012).
110. MAV (Municipal Archives of Vendôme). Antiphonarium, cum notis musicis XVth century. Latin Parchment, 229 folio: "...Quia cito veniet salus tua..." Notes relatives à des inondations survenues à Vendôme en 1342 (1459).
111. Isnard, I. *L'Abbatiale de la Trinité de Vendôme* (Rennes Univ. Press, 2007).
112. Matériaux du Monasticon gallicanum de Dom Germain. Latin 11821. https://archivesetmanuscrits.bnf.fr/ark:/12148/cc73258k Bibliothèque nationale de France. Département des Manuscrits. Latin 11821.
113. Plat, G. *L'église de la Trinité de Vendôme* (Laurens, 1934).
114. Herget, J. & Meurs, H. Reconstructing peak discharges for historic flood levels in the city of Cologne, Germany. *Glob. Planet Change* **70**, 108–116 (2010).
115. Schedel, H. *Liber chronicarum* (Nürnberg Koberger, 1493). Universitätstbibliothek Heidelberg. Digitale Bibliothek [M40784]; https://doi.org/10.11588/diglit.5223#0621.
116. Centralbureau für Meteorologie und Hydrographie im Großherzogthum Baden. *Der Rheinstrom und seine wichtigsten Nebenflüsse* (Selbstverlag, 1889).
117. Froning, R. *Frankfurter Chroniken und annalistische Aufzeichnungen des Mittelaters* (Jügel, 1884).
118. Bork, H.-R. & Kranz, A. Die Jahrtausendflut des Jahres 1342 prägt Deutschland. *Naturkunde* **158**, 119–129 (2008).

119. Boehmer, F. *Fontes rerum Germanicarum. Geschichtsquellen Deutschlands,* Erster Band (Cotta'scher, 1843).
120. Schiller, H. Ermittlung von Hochwasserwahrscheinlichkeiten am schiffbaren Main und überregionaler Vergleich der Ergebnisse. *Beit. Hydrol.* **S6**, 79–101 (1987).
121. Widmann, S. *Die Eberbacher Chronik der Mayenceer Erzbischöfe* (Hahn'sche Buchhandlung, 1888).
122. Roth, F.W.E. *Fontes rerum Nassoicarum. Geschichtsquellen aus Nassau,* Vol. 1: *Die Geschichtsquellen des Niederrheingaus* (Limbarth, 1880).
123. Ngo, H. et al. Reconstruction of the 1374 Rhine river flood event around Cologne region using 1D–2D coupled hydraulic modelling approach. *J. Hydrol.* **617**, 129039 (2023).
124. Van der Meulen, B., Defilet, M. P., Tebbens, L. A. & Cohen, K. M. Palaeoflood level reconstructions in a lowland setting from urban archaeological stratigraphy, Rhine river delta, the Netherlands. *Catena* **212**, 106031 (2022).
125. Pörtge, K.-H. & Deutsch, M. Hochwasser in Vergangenheit und Gegenwart. *Rundgespr. Ökol.* **18**, 139–151 (2000).
126. Gauger, M. in *Schauplätze und Themen der Umweltgeschichte* (eds Hermann, B. & Dahlke, C) 95–106 (Universitätsverlag, 2010).
127. Herget, J. et al. in *Die Thüringische Sintflut von 1613 und ihre Folgen für heute. Schriften der Deutschen Wasserhistorischen Gesellschaft 22* (ed. Ohlig, C.) 77–105. (Papierfliegerverlag, 2013).
128. Hindemith, A. Hochwassermarken Blasiuskirche. *Wikimedia* https://upload.wikimedia.org/wikipedia/commons/1/18/Hochwassermarken_Pfeiler_Blasiuskirche_M%C3%BCnden.jpg.
129. Schiltern D.J. *Die Alteste Teutsche so wol Allgemeine als inbesonderheit Elsassische und Straßburgische Chronicke. Von Jacob von Königshoven Priestern in Straßburg Von Anfang der Welt biß ins Jahr nach Christi Geburth MCCC LXXXVI beschrieben*. 365 (Städel, 1698).
130. *Topografische Karte Europa* (Topographicmap.com, accessed 23 February 2026); https://de-de.topographic-map.com/map-d71nx/Europa/.
131. Le service d'information sur le risqué de crues des principaux d'eau en France. *Vigicrues* http://www.vigicrues.gouv.fr/.
132. HydroPortail v3.4.5. Portail d'accès aux données hydrométriques et hydrologiques. *EauFrance* http://www.hydro.eaufrance.fr/.
133. Waton, M.-D. Les enceintes de Strasbourg à travers les siècles. *In Situ* **16**, 442 (2011).
134. Abdulkarim, M. et al. Morpho-sedimentary characteristics of Holocene paleochannels in the Upper Rhine alluvial plain, France. *E&G Quat. Sci. J.* **71**, 191–212 (2022).
135. Heinrich von Diessenhofen. *ALCUIN. Infothek der Scholastik* http://alcuin.de/philosopher.php?id=7126 (2026).
136. Merian, M. *Topographia Alsatiae completa*, Vol. 2 (Spörlin, 1643).
137. Bernouli, A. *Basler Chroniken,* Vol. 5; Vol. 6 (Hirzel, 1895; 1902).
138. Ott, H. (ed.) *Säckingen: Die Geschicte der Stadt* (Theiss, 1978).
139. Münster, S. *Cosmographei oder beschreibung aller laender herrschafften* (n.p., 1550); http://dl.ub.uni-freiburg.de/diglit/muenster1550.
140. Tilman2007. Lindau, Barfüßerplatz 1a. *Wikimedia* https://commons.wikimedia.org/wiki/File:Lindau,_Barf%C3%BC%C3%9Ferplatz_1a-004.jpg.
141. Kulturamt Lindau. Stadttheater Lindau, Außenansicht mit Eingang. *Wikipedia* https://de.wikipedia.org/wiki/Stadttheater_Lindau#/media/Datei:Au%C3%9Fenansicht_Eingang.jpg.
142. Bayerisches Landesamt für Umwelt. Umwelt Atlas Hochwasser. *Umwelt Atlas* https://www.umweltatlas.bayern.de/mapapps/resources/apps/umweltatlas/.
143. Ettmüller, L. *Die beiden ältesten Deutschen Jahrbücher der Stadt Zürich* (Meyer und Zeller, 1844).
144. Dierauer. J. (ed.) *Quellen zur Schweizer Geschichte*, Band 18 (Geering, 1900).
145. Merian, M. *Topographia Herveticae, Rhaetiae et Valesiae* (Matthaeus Merians Erben, 1642).
146. Wetter, O. & Specker, T. *HWS Sihl-Limmat –Schlussbericht Historische Studien* (AWEL, 2015).
147. Naef-Huber, D. et al. Hochwasserschutz Zürich – Seestände und Abfluss: Heute mit dem Schiff ins Zürher Fraumünster? *Wasser Energie Luft* **108**, 109–114 (2016).
148. Murer, H. Frauenfeld, Kantonsbibliothek Thurgau, Y 105: Chronicle of St. Katharinental, Töss and Berenberg Abbey, Ittingen. *Europeana* https://www.europeana.eu/en/item/92004/object_CHKBT_Y_105_____3ASVX63?page=59.
149. Grund Riss des Klosters zu Tös. 1780. *Zentralbibliothek Zürich*. https://www.e-manuscripta.ch/zuzneb/doi/10.7891/e-manuscripta-7174.
150. Hegel, K. *Die Chroniken der oberrheinischen Städte. 1. Straßburg*. 132–133 (Akademie, 1870).
151. Glunk, H. Beobachtungen an der Stadtmauer von Konstanz, Abschlussbericht der Rettungsgrabung (2023_0153): Konstanz „Bodanstraße 34". *Dok. Archäol. Baden-Württemberg* **14**, 1–11 (2025).
152. Kalt, N. Ansicht der Stadt Konstanz / Panorama of Konstanz. Staatliche Museen zu Berlin, Kupferstichkabinett (1601). https://id.smb.museum/object/1052499/ansicht-der-stadt-konstanz.
153. Konold, W. Die Regulierung des Bodensees: eine alte Geschichte. *Bürger & Staat* **50**, 82–86 (2000).
154. Dumitrache, M. *Die Konstanzer Markstätte im Mittelalter und in der Neuzeit* (Reichert, 2018).
155. Wessels, M., Mohaupt, K., Kümmerlin, R. & Lenhard, A. Reconstructing past eutrophication trends from diatoms and biogenic silica in the sediment and the pelagic zone of Lake Constance, Germany. *J. Paleolimnol.* **21**, 171–192 (1999).
156. Gunten, H. R. et al. Sedimentation rates in the central Lake Constance determined with ^{210}Pb and Cs. *Schweiz. Z. Hydrol.* **49**, 275–283 (1987).
157. Schaller, S. et al. Postglacial evolution of Lake Constance: sedimentological and geochemical evidence from a deep-basin sediment core. *Swiss J. Geosci.* **115**, 7 (2022).
158. Merle, W. *Consideraciones temperiei pro septem annis Christi. The earliest known journal of the weather* (ed. Symons, G. J.) 1337–1344 (Stanford, 1891).
159. van Bebber, W. J. Die Zugstrassen der barometrischen Minima nach den Bahnenkarten der Deutschen Seewarte für den Zeitraum 1875-1890. *Meteorol. Z.* **8**, 361–466 (1891).
160. Young, G. H. et al. Changes in atmospheric circulation and the Arctic Oscillation preserved within a millennial length reconstruction of summer cloud cover from northern Fennoscandia. *ClimDyn* **39**, 495–507 (2012).
161. Bologna, Archivio de Stato, Comune – Governo – Signoria Pepoli: Provvigioni cartacea 236, f. 115 v.
162. Jóźwiak, S. in *Studies on the Military Orders, Prussia, and Urban History* (eds Jarnowsky, K. et al.) 261–272 (Univ. Debrecen 'Hungary in Medieval Europe' Research Group, 2020).
163. Bauch, M. & Forster, C. in *Pilgern zu Wasser und zu Lande*. Jakobus-Studien 24 (eds Kühne, H. & Popp, C.) 15–78 (Narr Francke Attempto Verlag, 2022).
164. Gajdošová, J. Imperial memory and the Charles Bridge. *Ostblick* **3**, 1–11 (2012).
165. Nagel, W. *Die alte Dresdner Augustusbrücke* (Verein für Geschichte Dresdens, 1924).
166. Privilege and permission charter issued by Pope Clemens VI to the Abbess of the St. Fridolin Nunnery (Fridolinmünster), Säckingen; 30 September 1345. Landesarchiv Baden-Württemberg, Generallandesarchiv Karlsruhe, 16: Säckingen, Urkunden. Papal register No.: AAV, Reg. Vat. 172, f° 172r–v.
167. Lorenc, V. *Das Prag Karls IV. Die Prager Neustadt* (Deutsche Verlagsanstalt, 1982).
168. Graus, F. in *Zentralität als Problem der mittelalterlichen Stadtgeschichtsforschung* (ed. Meynen, E.) Städteforschungen Reihe A: Darstellungen Bd. 8 (Böhlau, 1979).
169. Gedeon, L. Prozessionen in Frankfurt am Main. *Arch. Mittelrheinisch. Kirchengesch. Nebst Ber. Kirchlichen Denkmalpfl.* **52**, 11–54 (2000).
170. Blischke, D. Vor uns die Sintflut – Zur Krisenbewältigung des Magdalenenhochwassers 1342 an ausgewählten Fallbeispielen. *Mittelalter* **4**, 33–50 (2021).
171. Shepherd, W. R. *Historical Atlas* (Holt and Company, 1911).
172. Herbert, Cl.-J. in *Essai sur la police générale des grains, sur leurs prix et sur les effets de l'agriculture 1755* (ed. Depitré, E.) 76–78 (Geuthner, 1910).
173. Usher, A. P. The general course of wheat prices in France: 1350–1788. *Rev. Econ. Stat.* **12**, 162 (1930).
174. Bauernfeind, W. *Materielle Grundstrukturen im Spätmittelalter und der Frühen Neuzeit* (Schriftreihe des Stadtsarchivs Nürnberg, 1993).
175. Slavin, P. *Bread and Ale for the Brethen: The Provisioning of Norwich Cathedral Priory, 1260–1536* (Univ. Hertfordshire Press, 2012).
176. Vulliod, F. *La Normandie occidentale (la Manche) de la fin du Moyen Age au milieu du XIX siècle: étude démographique et économique.* PhD thesis, Normandie Univ. (2018).
177. Espeel, S. Driven by crises: price integration on the grain market in late medieval Flanders. *Econ. Hist. Rev.* **77**, 849–872 (2024).
178. Phelps-Brown, E. H. & Hopkins, S.hV. Seven centuries of the price of consumables, compared with builders' wage rates. *Economica* **23**, 296–314 (1956).
179. Munro, J. H. *Database of 'Seven centuries of the price of consumables, compared with builders' wage rates of Phelps-Brown, E.H. & Hopkins, S.V.'* (corrected and converted by Munro, J.) https://www.economics.utoronto.ca/munro5/ResearchData.html (2012).
180. Hybel, N. The grain trade in Northern Europe before 1350. *Econ. Hist. Rev.* **55**, 219–247 (2002).
181. Continuatio Novimontensis. in *Monumenta Germaniae Historica.* Scriptores, Vol. 9 (ed. Wattenbach, W.) 688–677 (Hahn, 1851).
182. Espeel, S. The grain market and preferential trade of large landowners in Flemish cities during the Age of Shocks (1330–1370). *MEFRM* **131**, 29–44 (2019).
183. Galloway, J. A. One market or many? London and the grain trade of England. *CMH Work. Pap. Ser.* **3**, 23–42 (2000).
184. Campbell, B. in *Le interazioni fra economia e ambiente biologico nell'Europe preindustriale. Secc. XIII-XVIII/Economic and Biological Interactions in Pre-Industrial Europe from the 13th to the 18th Centuries* (ed. Cavaciocchi, S.) 13–32 (Florence Univ. Press, 2010).
185. Farmer, D. L. in *The Agrarian History of England and Wales*, Vol 2, 1042–1350. (ed. Hallam, H. E.) 716–817 (Cambridge Univ. Press, 1988).
186. Medieval English Grain Yield Database. https://jordanclaridge.com/datasets (2026).
187. Mäesalu, M. Taani kuninga asehaldur Konrad Preen ja Jüriöö ülestõus. *Tuna* **2**, 9–24 (2021).
188. Kiss, A., Piti, F., Sebők, F. & Teiszler, É. in *The Crisis of the 14th Century. Teleconnections between Environmental and Societal Change?* (eds Bauch, M. & Schenk, G.) 100–129 (De Gruyter, 2020).
189. Piti, F. *Anjou-kori oklevéltár / Documenta res Hungaricas tempore regum Andegavensium illustrantia*, Vols. 26, 27 (1342, 1343) (Szegedi Középkorász Műhely, 2007).
190. Ravančić, G. Economic activities of Dubrovnik during the plague epidemics in the fourteenth century. *Hist. Zb.* **77**, 43–55 (2024).
191. Morrison, C. & Cheynet, J.-C. in *The Economic History of Byzantium: From the Seventh through the Fifteenth Century* (eds Laiou, A. E. et al.) 815–878 (Dumbarton Oaks, 2002).
192. L'Istorie e l'arme delle Famiglie più antiche di Venezia, c 194v, Ms. anonimo, Venezia, Bibl. Museo Correr, Cod. Gradenigo 131, cc. 206.
193. Müller, R. C. *The Venetian Money Market: Banks, Panics, and the Public Debt, 1200–1500* (Johns Hopkins Univ. Press, 2019).
194. de La Roncière, C.-M. *Prix et salaires à Florence au XIVe siècle (1280–1380)* (Publications de l'École française de Rome, 1981).
195. Dameron, G. Feeding the medieval Italian City-state. *Speculum* **92**, 976–1019 (2017).
196. Nanni, P. in *The Crisis of the 14th Century* (eds Bauch, M. & Schenk, G.) 169–189 (De Gruyter, 2020).
197. Larenaudie, M.-J. Les famines en Languedoc aux XIVe et XVe siècles. *Ann. Midi* **64**, 27–39 (1952).
198. Melis, A.R. *Els cereals i el pa en els països de llengua catalana a la baixa edat mitjana* (Institut d'Estudis Catalans, 2017).
199. Melis, A.R. *Alimentación, sociedad, cultura y política en el Occidente medieval* (Ediciones Trea, 2021).
200. Hamilton, E.J. *Money, Prices, and Wages in Valencia, Aragon, and Navarre 1351–1500* (Porcupine Press, 1975).
201. Faigl, M. *Die Urkunden des Regulierten Chorherrensstiftes Herzogenburg vom Jahre seiner Übertragung von St. Georgen: 1244 bis 1450* (Mayer, 1886).
202. Wenzel, G. *Magyar Diplomácziai Emlékek az Anjou-korból II* (Magyar Tudományos Akadémia, 1875).
203. Thompson, M. E. *Adeae Murimuth Continuatio Chronicarum* (Cambridge Univ. Press, 2012).

204. Bond, E.A. *Chronica Monasterii de Melsa a fundatione usque ad annum 1396* (Longmans, 1868).
205. Venezia, Archivio di Stato, Senato Misti, reg. 20, 5 Aug. 1342.
206. Bologna, Archivio di Stato, Comune – Governo – Signoria Pepoli: Provvigioni cartacea 238 (1342–1343), Vol. II-19, f. 56r.
207. Bologna, Archivio di Stato, Comune – Governo – Signoria Pepoli: Provvigioni cartacea 239 (1343), Vol. II-22, f. 74r.–78v.
208. Alexandre, P. *Le climate en Europe au Moyen Age, contribution à l'histoire ds variations climatiques de 1000 à 1425, d' après les sources narratives de l'Europe occidentale* (École des hautes études en sciences sociales, 1987).
209. Champion, M. *Les inundations en France depuis le VIe siècle jusqu'a nos jours* (Dunod, 1858–1863).
210. Weikinn, C. *Quellentexte zur Witterungsgeschichte Europas von der Zeitwende bis zum Jahre 1850: Hydrographie*, Vols. 1–6 (Akademie Verlag, 1958–2002).
211. Glaser, R. *Klimageschichte Mitteleuropas: 1200 Jahre Wetter, Klima, Katastrophen* (Primus Verlag, 2013).
212. Telelis, I. G. Climatic fluctuations in the Eastern Mediterranean and the Middle East AD 300–1500 from Byzantine documentary and proxy physical paleoclimatic evidence – a comparison. *Jahrb. Österr. Byzantinistik* **58**, 167–207 (2008).
213. Lászlóffy, W. *A Tisza* (Akadémiai Kiadó, 1982).
214. Tuncok, I. K. Transboundary river basin flood forecasting and early warning system experience in Maritza River basin between Bulgaria and Turkey. *Nat. Hazards* **75**, 191–214 (2014).
215. Simonová, D., Holubecká, M. & Jarošová, M. *Povodnová situácia na východnom Slovensku v novembri 2009. Slovenský hydrometeorologický ústav. Odbor Hydrologické predpovede a výstrahy Košice* (SHMÚ, 2009).
216. Simonová, D., Holubecká, M., Jarošová, M. & Smrtník, P. *Povodňová situácia na východnom Slovensku v decembri 2009 a v januári 2010. Slovenský hydrometeorologický ústav. Odbor Hydrologické predpovede a výstrahy Košice* (SHMÚ, 2010).
217. *Megemlékezés a 2010. évi Észak-magyarországi árvizekről* (EMVIZIG, 2010).
218. *Past weather in Budapest, Hungary – December 2009* (Timeanddate, accessed 31 August 2025); https://www.timeanddate.com/weather/hungary/budapest/historic?month=12&year=2009.
219. *Past weather in Budapest, Hungary – January 2010* (Timeanddate, accessed 31 August 2025); https://www.timeanddate.com/weather/hungary/budapest/historic?month=1&year=2010.
220. *Monthly precipitation total in January 2010* (Deutsche Wetterdienst, accessed 21 September 2025); https://www.dwd.de/EN/ourservices/rcccm/int/rcccm_month_rrr.html.
221. *Monthly sea level pressure: January 2010 in comparison with the 1961-1990 means* (Deutsche Wetterdienst, accessed 21 September 2025); https://www.dwd.de/EN/ourservices/rcccm/int/rcccm_month_rrr.html.
222. *Hydrological Reports: Flood reports 2009–2010* (SHMÚ, accessed 31 August 2025); https://www.shmu.sk/en/?page=1&id=mim_hydro_sprav&rok=2010&mesiac=1&sending=.
223. *Climatological Services 2009–2010: Precipitation* (SHMÚ, accessed 31 August 2025); https://www.shmu.sk/en/?page=1&id=klimat_operativneudaje2&identif=11816&rok=2010&obdobie=1991-2020.
224. Blahová, A. et al. *Správa o povodniach za rok 2010. Slovenský Hydrometeorologický Ústav. Centrum predpovedí a výstrah Odbor Hydrologické predpovede a výstrahy* (SHMÚ, 2011).
225. Poulos, S. et al. An Insight into the factors controlling delta flood events: the case of the Evros River deltaic plain (NE Aegean Sea). *Water* **14**, 497 (2022).
226. Pichard, G., Arnaud-Fassetta, G., Moron, V. & Roucaute, E. Hydro-climatology of the Lower Rhône Valley: historical flood reconstruction (AD 1300–2000) based on documentary and instrumental sources. *Hydrol. Sci. J.* **62**, 1772–1795 (2017).
227. ICPDR Flood Protection Expert Group. *The analysis of the Danube Floods 2006* (ICPDR, 2007).
228. Thielen, J. et al. *European Flood Alert System 4th Annual Report 2006* (Ispra JRC RC 2007).
229. Younis, J., Ramos, M.-H. & Thielen, J. EFAS forecast for the March–April 2006 flood in the Czech part of the Elbe River Basin—a case study. *Atmos. Sci. Lett.* **9**, 88–94 (2008).
230. Twardosz, R., Kossowska-Czezak, U. & Pelech, S. Extremely cold winter months in Europe (1951–2010). *Acta Geophys.* **64**, 2609–2629 (2016).
231. EUCOLD Working Group on Levees and Flood Defences July 2018. *European and US Levees and Flood Defences. Characteristics, Risks and Governance* (CFBR, 2019).
232. *NOAA reanalysis maps: 500 hPa geopotential height (27–29 March)* (Wetterzentrale, accessed 4 April 2026); https://www.wetterzentrale.de/reanalysis.php?jaar=2006&maand=3&dag=27&uur=1800&var=1&map=1&model=noaa.
233. *Előzetes kockázatbecslés országjelentése. A jelentés a 2007/60/EK Irányelve alapján készült* (KÖTIVIZIG, 2012); https://www.kotikovizig.hu/doksik/akk/elozetes_kockazatbecsles_orszagjelentes.pdf.
234. Civil Protection. Floods spring 2006. *European Commission* https://ec.europa.eu/echo/files/civil_protection/floods_2006.htm.
235. Tisza: Vásárosnamény. *Központi Hidrológiai Adattár. Archívum (KHAA)*; https://www.hydroinfo.hu/vituki/archivum/vn.htm.
236. Tisza: Szolnok. *Központi Hidrológiai Adattár. Archívum (KHAA)*; https://www.hydroinfo.hu/vituki/archivum/so.htm.
237. *Climate monitoring Europe – Maps of precipitation (monthly values) – WMO RA VI region. Monthly precipitation total in March 2006* (Deutsche Wetterdienst, accessed 21 September 2025); https://www.dwd.de/EN/ourservices/rcccm/int/rcccm_month_rrr.html;jsessionid=59F9D408BDC2585628C8D3CE28A21179.live21062?nn=790954.
238. Homokiné Újváry, K. & Kalmár, Gy. Tavaszi ár a Dunán és a Tiszán 2006. *Országos Meteorológiai Szolgálat* http://owww.met.hu/pages/arviz20060614.php.
239. *Report on April 2006 floods in South Eastern Europe* (OCHA Services, reliefweb; 2006); https://reliefweb.int/report/hungary/report-april-2006-floods-south-eastern-europe.
240. *2006 floods in the Danube River Basin. Flood risk mitigation for people living along the Danube: the potential for floodplain protection and restoration. Working paper. Vienna, July 2006* (WWF EU, 2006); https://wwfeu.awsassets.panda.org/downloads/2006_floods_in_the_danube_river_basin_wwf_working_paper.pdf.
241. *Climate monitoring Europe – Maps of precipitation (monthly values) – WMO RA VI region. Monthly precipitation total in April 2006* (Deutscher Wetterdienst (DWD), accessed 21 September 2025); https://www.dwd.de/EN/ourservices/rcccm/int/rcccm_month_rrr.html.
242. *NatRisk project. Report on natural disasters in the Western Balkans. Development of master curricula for natural disasters risk management in Western Balkan countries (573806-EFP-1-2016-1-RS-EPPKA2-CBHE-JP), 2016* (NatRisk, 2017); http://www.natrisk.ni.ac.rs/files/activities/1-1/Report_on_natural_disasters_in_WB.pdf.
243. Vidmar, A. The Bosna River floods in May 2014. *Nat. Hazards Earth Syst. Sci.* **16**, 2235–2246 (2016).
244. Tolika, K., Maheras, P. & Anagnostopoulou, C. The exceptionally wet year of 2014 over Greece: statistical and synoptical–atmospheric analysis over the region of Thessaloniki. *Theor. Appl. Climatol.* **132**, 809–821 (2018).
245. Stadtherr, L. et al. Record Balkan floods of 2014 linked to planetary wave resonance. *Sci. Adv.* **2**, e1501428 (2016).
246. Cook, E. R. et al. Old World megadroughts and pluvials during the Common Era. *Sci. Adv.* **1**, e1500561 (2015).
247. Tegel, W. et al. Higher groundwater levels in Western Europe characterize warm periods in the Common Era. *Sci. Rep.* **10**, 16284 (2020).
248. Krug, A., Aemisegger, F., Sprenger, M. & Ahrens, B. Moisture sources of heavy precipitation in Central Europe in synoptic situations with Vb-cyclones. *Clim. Dyn.* **59**, 3227–3245 (2022).
249. Luterbacher, J. European summer temperatures since Roman times. *Environ. Res. Lett.* **11**, 024001 (2016).
250. Proctor, C., Baker, A. & Barnes, W. L. A three thousand year record of North Atlantic climate. *Clim. Dyn.* **19**, 449–454 (2002).
251. Deutsches Komitee Katastrophenvorsorge. *Das Hochwasser im Juni 2013. Bewährungsprobe für das Hochwasserrisikomanagement in Deutschland. DKKV-Schriftenreihe 53* (DKKV, 2015).
252. Merz, B., Nguyen, V. D. & Vorogushyn, S. Temporal clustering of floods in Germany: do flood-rich and flood-poor periods exist? *J. Hydrol.* **541**, 824–838 (2016).
253. Mohr, S. et al. A multi-disciplinary analysis of the exceptional flood event of July 2021 in central Europe – Part 1: Event description and analysis. *Nat. Hazards Earth Syst. Sci.* **23**, 525–551 (2023).
254. Ludwig, P. et al. A multi-disciplinary analysis of the exceptional flood event of July 2021 in central Europe – Part 2: Historical context and relation to climate change. *Nat. Hazards Earth Syst. Sci.* **23**, 1287–1311 (2023).
255. Roth, R. Einige Bemerkungen zur Entstehung von Sommerhochwasser aus meteorologischer Sicht. *Z. Kulturtech.* **37**, 241–245 (1996).
256. Bork, H.-R. *Landschaften der Erde unter dem Einfluss des Menschen* (Primus, 2006).
257. Wyttenbach, J.H. & Müller, M.F.J. *Gesta Trevirorum. Vol. 2: Ab anno MCCLIX usque ad mortem archiepiscopi Richardi a Greifenclau anno MDXXXI* (Lintz, 1838).
258. Merz, B. et al. Charting unknown waters—on the role of surprise in flood risk assessment and management. *Water Resour. Res.* **51**, 6399–6416 (2015).
259. Messmer, M., Gómez-Navarro, J. J. & Raible, C. C. Climatology of Vb cyclones, physical mechanisms and their impact on extreme precipitation over Central Europe. *Earth Syst. Dyn.* **6**, 541–553 (2015).
260. Roggenkamp, T., Herget, J. & Roggenkamp, T. Flood reconstruction—the unexpected rather frequent event at River Ahr in July 2021. *Glob. Planet Change* **240**, 104541 (2024).
261. Vorogushyn, S. It could have been much worse: spatial counterfactuals of the July 2021 flood in the Ahr Valley, Germany. *Nat. Hazards Earth Syst. Sci.* **25**, 2007–2029 (2025).
262. Blöschl, G. The June 2013 flood in the Upper Danube Basin, and comparisons with the 2002, 1954 and 1899 floods. *Hydrol. Earth Syst. Sci.* **10**, 9533–9573 (2013).
263. *Past Weather in Hertford, England, United Kingdom—August 2021* (Timeanddate, accessed 12 October 2025); www.timeanddate.com/weather/@2647044/historic?month=8&year=2021.
264. Petrić, H. in *Man, Nature and Environment Between the Northern Adriatic and the Eastern Alps in Premodern Times* (eds Štih, P. & Zwitter, Ž.) 260–289 (Znanstvena založba Filozofske fakultete Univerze v Ljubljani, 2014).
265. Laczko, M., Potočki, K., Škreb, K. A. & Beza, N. Joint modelling of flood hydrograph peak, volume and duration using copulas – Case study of Sava and Drava River in Croatia, Europe. *Water* **14**, 2481 (2022).
266. Caporali, E., Rinaldi, M. & Casagli, N. The Arno River floods. *Giorn. Geol. Appl.* **1**, 177–192 (2005).
267. Pont, D., Day, J. W. & Ibáñez, C. The impact of two large floods (1993–1994) on sediment deposition in the Rhône delta: implications for sustainable management. *Sci. Total Environ.* **609**, 251–262 (2017).
268. Stucki, P., Martius, O., Brönnimann, S. & Franke, J. The extreme flood event of Lago Maggiore in September 1993. *Geogr. Bern* **G89**, 53–58 (2013).
269. Malguzzi, P., Grossi, G., Buzzi, A., Ranzi, R. & Buizza, R. The 1966 'century' flood in Italy: a meteorological and hydrological revisitation. *J. Geophys. Res.* **111**, D24106 (2006).
270. Ormánsági História. A nagy drávai árvíz - 1972. *Ormánsági Krónika* https://ormansagihistoria.blog.hu/2018/11/22/a_nagy_dravai_arviz (22 November 2022).
271. Schubert, J. et al. Vízgazdálkodás a Dél-dunántúli Vízügyi Igazgatóság működési területén. *Hidrol. Közlöny* **100**, 5–17 (2020).
272. The Italian floods of May 2023: a scientific analysis. *CIMA Research Foundation* https://www.cimafoundation.org/en/news/the-italian-floods-of-may-2023-a-scientific-analysis/ (2023).
273. *October weather in Algeciras, Spain* (Weather Spark, accessed 6 September 2025); https://weatherspark.com/m/34142/10/Average-Weather-in-October-in-Algeciras-Spain.
274. Wet end to the year in western and southern Europe. *ESOTC Copernicus Climate Change Service* https://climate.copernicus.eu/ESOTC/2019/wet-end-year-western-and-southern-europe (2019).
275. Gil-Guirado, S. et al. Flood impact on the Spanish Mediterranean coast since 1960 based on the prevailing synoptic patterns. *Sci. Total Environ.* **807**, 150777 (2022).
276. DANA storm system causes major flooding throughout Spain. *Project44* https://www.project44.com/supply-chain-insights/dana-storm-system-causes-major-flooding-through-spain/ (2024).
277. Fekete, A., Estrany, J. & Ramírez, M.ÁA. Cascading impact chains and recovery challenges of the 2024 Valencia catastrophic floods. *Discov. Sustain.* **6**, 586 (2025).

278. Meneguzzo, F. et al. Sensitivity of meteorological high-resolution numerical simulations of the biggest floods occurred over the Arno river basin, Italy, in the 20th century. *J. Hydrol.* **288**, 37–56 (2004).
279. Tisza: Szeged. *Központi Hidrológiai Adattár. Archívum (KHAA)* https://www.hydroinfo.hu/vituki/archivum/se.htm.
280. Alberoni, P. P. et al. Mesoscale analysis of the October 1998 Friauli flood event. In *Proc. 2nd EGS Plinius Conference on Mediterranean Storms* (eds Mugnai, A. et al.) 1–11 (EGS, 2000).
281. Nagy, B. et al. *A Felső-tiszai árvizek kialakulásának tényezői, különös tekintettel az utóbbi évek katasztrófáira, illetve azok elhárításának lehetőségeire* (Berehove, 2002).
282. Draper, L. & Bownass, T.M. Unusual waves on European Coasts, February 1979. In *Proc. 18th Coastal Engineering Conference* (ed. Edge, B. L.) 270–281 (American Society of Civil Engineers, 1982).
283. Draper, L. & Bownass, T. M. Wave devastation behind Chesil Beach. *Weather* **38**, 346–352 (1983).
284. Sibley, A. & Cox, D. Flooding along English Channel coast due to long-period swell waves. *Weather* **69**, 59–66 (2014).
285. Szlávik, L. A 2001. évi felső-tiszai árvíz kialakulása és hidrológiai sajátosságai. *Vízügyi Közl Különszám* **3**, 13–34 (2003).
286. *Historical weather 2001 in Algeciras, Spain. Wind direction, wind speed* (Weather Spark, accessed 15 September 2025); https://weatherspark.com/h/y/34142/2001/Historical-Weather-during-2001-in-Algeciras-Spain#Figures-WindDirection.
287. Bodolainé Jakus, E. & Táncz, T. A 2001. márciusi hirtelen tiszai árhullám meteorológiai háttere. *Légkör* **50**, 2–11 (2005).
288. European Centre for Medium-Range Weather Forecasts. 201703 – Windstorm – Zeus https://confluence.ecmwf.int/display/FCST/201703+-+Windstorm+-+Zeus.
289. Fabricius, G. *Rerum Miscinarum Libri VII* (ed. Borsch, J. B.) (Voegelinus, 1569).
290. Güth, J.M.S. *Poligraphia Meiningensis, Das ist Gründliche Beschreibung Der Uhr-alten Stadt Meiningen* (Reyhern, 1676).
291. Klemm, G.F. *Die Geschichte Dresdens von 1827 Chronik der Königlich Sächsischen Residenzstadt Dresden*, Vol. 1 (SLUB, 1840).
292. Vágási, I. Folyók tetőző vízállásainak haladása az árhullámban. *Hidrol. Közlöny* **80**, 45–53 (2000).
293. Laczi, Z. 25 éve vonult le az évszázad árvize. *Közép-Tisza Vidéki Vízügyi Igazgatóság* https://www.kotivizig.hu/kozep-tisza-videki/hireink/ovf-hirek/25-eve-vonult-le-az-evszazad-arvize (2025).
294. Homokiné Ujváry, K. Márciusi árvíz Kárpátalján. *Légkör* **46**, 2–6 (2001).
295. Homokiné Ujváry, K. A víz az úr? *Légkör* **45**, 24–28 (2000).
296. Homokiné Ujváry, K. A medárdi negyven nap. *Légkör* **44**, 2–5 (1999a).
297. Homokiné Ujváry, K. Őszi árvíz a Tiszán. *Légkör* **44**, 2–6 (1999b).
298. Domonkos, P. et al. Az 1999. évi belvizek kialakulásának okai. *Légkör* **45**, 11–16 (2000).
299. Bezzola, G. R & Hegg, C. *Ereignisanalyse Hochwasser 2005. Teil 2 – Analyse von Prozessen, Massnahmen und Gefahrengrundlagen* (BAFU, 2008).
300. Department for the Environment, Transport, Energy and Communications. *The Floods of 2005 in Switzerland. Synthesis Report on the Event Analysis* (FOEN, 2008).
301. Joehnk, K., Straile, D. & Ostendorp, W. Water level variability and trends in Lake Constance in the light of the 1999 centennial flood. *Limnologia* **34**, 15–21 (2004).
302. Grieser, J., Beck, C. & Brázdil, R. The summer flooding 2005 in Southern Bavaria—a climatological review. *Deutsch. Wetterdienst* **16**, 168–173 (2005).
303. Stucki, P. et al. Weather patterns and hydro-climatological precursors of extreme floods in Switzerland since 1868. *Meteorol. Z.* **21**, 531–550 (2012).
304. Kautz, L.-A. et al. Atmospheric blocking and weather extremes over the Euro–Atlantic sector: a review. *Weather Clim. Dyn.* **3**, 305–336 (2022).
305. Sieber, A. et al. *Ermittlung des Extremwasserstandes (ca. HW1000) für den Bodensee (Ober- und Untersee)* (LUBW-BAFU-VW, 2011).
306. Näef-Huber, D. et al. Hochwasserschutz Zürich – Seestände und Abfluss: Heute mit dem Schiff ins Zürcher Fraumünster? *Wasser Energie Luft* **108**, 109–114 (2016).
307. Bernoulli, A. *Basler Chroniken*, Vol. 5 (Hirzel, 1895).
308. Bernoulli, A. *Basler Chroniken*, Vol. 6 (Hirzel, 1902).
309. Schaller-Donauer, A. *Chronik der Naturereignisse im Urnerland 1000–1800* (Gotthardpost, 1938).
310. Klemm, F. *Die Entwicklung der meteorologischen Beobachtungen in der Schweiz bis zum Jahre 1700* (Leeman, 1974).
311. Tschamser, M. *Annales oder Jahrs-Geschichten der Baarfüseren oder Minderen Brüdern S. Franc. ord., insgemein Conventualen genannt, zu Thann* (Hoffman, 1864).
312. Cook, B. I., Cook, E. R., Anchukaitis, K. & Singh, D. Characterizing the 2010 Russian heat wave–Pakistan flood concurrent extreme over the last millennium using the Great Eurasian Drought Atlas. *J. Clim.* **37**, 4389–4401 (2024).
313. Hennegriff, W. & Wahl, B. *Langzeitverhalten der Bodensee-Wasserstände. Auswertezeitspanne: 1888 bis 2007. Landesanstalt für Umwelt, Messungen und Naturschutz Baden-Württenberg* (LUBW, 2011).
314. Ansell, T. et al. Daily mean sea level pressure reconstructions for the European—North Atlantic region for the period 1850–2003. *J. Clim.* **19**, 2717–2742 (2006).
315. Rössler, O. & Brönimann, S. The effect of the Tambora eruption on Swiss flood generation in 1816/1817. *Sci. Total Environ.* **627**, 1218–1227 (2018).
316. Kiss, A. Weather and weather-related natural hazards in medieval Hungary III: documentary evidence on the 14th century. *Medium Aev. Quotid.* **73**, 5–55 (2016).
317. What is anticyclonic gloom? *UK Met Office* https://www.metoffice.gov.uk/blog/2025/what-is-anticyclonic-gloom (2025).
318. Micle, S. The variation of temperature and rainfall in the municipality of Cluj-Napoca in the interval 1979–2019. *Sci. Pap. Ser. E* **9**, 141–146 (2020).
319. *Cluj-Napoca 1984* (TuTiempo, accessed 25 October 2025); https://en.tutiempo.net/climate/1984/ws-151200.html.
320. *September 1984, the course of weather at the Cluj International Airport. Daily weather observations* (Weather Spark, accessed 25 October 2025); https://de.weatherspark.com/h/m/148515/1984/9/Historisches-Wetter-im-September-1984-am-Cluj-Napoca-International-Airport-Rum%C3%A4nien.
321. *Near-surface and sea-surface temperature anomalies, September 1984* (Copernicus Climate Plus, accessed 27 October 2025); https://pulse.climate.copernicus.eu/.
322. Fazekas, L. et al. *Upper Tisza flood November 1998* (VIZITERV, 2001).
323. Pekarova, P. et al. Disaster flood scenario: case study of the Uh River at Lekárovce (Slovakia). *IOP Conf. Ser. Earth Environ. Sci.* **906**, 012102 (2021).
324. Homokiné Újvári, K. Az 1998. novemberi tiszai árvíz meteorológiai jellemzése. Vízügyi Közlemények **1**, 35–49 (2003).
325. Chipak, V. P., Illés, L. & Nagy, L. Árvíz Ukrajnában 1998 novemberében. Vízügyi Közlemények **1**, 105–110 (2003).
326. Gauzer, B. & Bartha, P. Árvízi szimulációs vizsgálatok a Felső-Tiszán az 1998. novemberi árhullám alapján. Vízügyi Közlemények **1**, 93–104 (2003).
327. Konecsny, K. A Felső-Tisza 1998-2001 évi árvizeinek hidrológiai értékelése. *Hidrol. Közlöny* **83**, 75–86 (2003).
328. *1990 weather history in Gibraltar. Daily weather observations; wind speed data* (Weather Spark, accessed 3 September 2025); https://weatherspark.com/h/y/34081/1990/Historical-Weather-during-1990-in-Gibraltar.
329. *1998 weather history in Gibraltar. Daily weather observations; (Daily) wind speed data* (Weather Spark, accessed 3 September 2025); https://weatherspark.com/h/y/34081/1990/Historical-Weather-during-1998-in-Gibraltar.
330. *Near-surface and sea-surface temperature anomalies, November 1984* (Copernicus Climate Plus, accessed 27 October 2025); https://pulse.climate.copernicus.eu/.
331. Illés, L., Konecsny, K., Kovács, S. & Szlávik, L. Az 1998. novemberi árhullám hidrológiája. Vízügyi Közlemények **1**, 47–76 (2003).
332. Bodolainé Jakus, E. Az 1998. évi őszi tiszai és más nagy árhullámok időjárási okairól. Vízügyi Közlemények **1**, 21–33 (2003).
333. Huang, T. et al. Synoptic background conditions and moisture transport for producing the extreme heavy rainfall event in Valencia in 2024. *Atmos. Ocean. Sci. Lett.* **18**, 100666 (2025).
334. Alfaro-Sánchez, R. A. et al. Climatic and volcanic forcing of tropical belt northern boundary over the past 800 years. *Nat. Geosci.* **11**, 933–938 (2018).
335. Phipps, S. J. et al. Paleoclimate data-model comparison and the role of climate forcings over the past 1500 years. *J. Clim.* **26**, 6915–6936 (2013).
336. Ortega, P. et al. A model-tested North Atlantic Oscillation reconstruction for the past millennium. *Nature* **523**, 71–74 (2015).
337. Crowley, T. J. & Unterman, M. B. Technical details concerning development of a 1200-yr proxy index for global volcanism. *Earth Syst. Sci. Data* **5**, 187–197 (2013).
338. Kobashi, T. et al. On the origin of the multidecadal to centennial Greenland temperature anomalies over the past 800 yr. *Clim. Past* **9**, 583–559 (2013).
339. Kinnard, C. Reconstructed changes in Arctic Sea ice over the past 1,450 years. *Nature* **479**, 509–512 (2011).
340. Sigl, M. et al. Volcanic stratospheric sulfur injections and aerosol optical depth during the Holocene (past 11 500 years) from a bipolar ice-core array. *Earth Syst. Sci. Data* **14**, 3167–3196 (2022).
341. Hutchison, W. et al. High-resolution ice-core analyses identify the Eldgjá eruption and a cluster of Icelandic and trans-continental tephras between 936 and 943 CE. *JGR Atmos.* **129**, e2023JD040142 (2024).
342. Brázdil, R. et al. European floods of the winter 1783/84: scenarios of an extreme event during the 'Little Ice Age.' *Theor. Appl. Climatol.* **100**, 163–189 (2010).
343. Steiger, N. J., Smerdon, J. E., Cook, E. R. & Cook, B. I. A reconstruction of global hydroclimate and dynamical variables over the Common Era. *Sci. Data* **5**, 180086 (2018).
344. Tardif, R. et al. Last millennium reanalysis with an expanded proxy database and seasonal proxy modeling. *Clim. Past* **15**, 1251–1273 (2019).
345. Storm, G. *Islandske Annaler Indtil 1578* (Christiania Udgivne for det norske historiske kildeskriftfond, 1888).
346. Hermannsson, H. *Annalium in Islandia Farrago and De Mirabilibus Islandiae by Gísli Oddsson. Islandica X*, Vol. 2. (Cornell Univ., 1916).
347. Hoshizumi, H. & Miyabuchi, Y. *Volcanoes: 84. Asosan* (Japan Meteorological Agency, Data Centre); https://www.data.jma.go.jp/vois/data/filing/souran_eng/volcanoes/084_asosan.pdf.
348. Þórarinsson, S. Neðansjávargos við Ísland. *Natturufraedingurinn* **35**, 49–74 (1965).
349. Westercamp, D. & Traineau, H. The past 5,000 years of volcanic activity at Mt. Pelle Martinique (F.W.I.): implications for assessment of volcanic hazards. *J. Volcanol. Geotherm. Res.* **17**, 159–185 (1983).
350. Boudon, G. & Balcone-Boissard, H. Volcanological evolution of Montagne Pelée (Martinique): a textbook case of alternating Plinian and dome-forming eruptions. *Earth Sci. Rev.* **221**, 103754 (2021).
351. Wu, B., Wang, J. & Walsh, J. E. Dipole anomaly in the winter Arctic atmosphere and its association with sea ice motion. *J. Clim.* **19**, 210–225 (2006).
352. Keylock, C. J. The North Atlantic Oscillation and snow avalanching in Iceland. *Geophys. Res. Lett.* **30**, 1254 (2003).
353. DallaSanta, K., Gerber, E. P. & Toohey, M. The circulation response to volcanic eruptions: the key roles of stratospheric warming and eddy interactions. *J. Clim.* **32**, 1101–1120 (2019).
354. Emile-Geay, J., Seager, R., Cane, M. A., Cook, E. R. & Haug, G. H. Volcanoes and ENSO over the past millennium. *J. Clim.* **21**, 3134–3148 (2008).
355. Gao, Y. & Gao, C. European hydroclimate response to volcanic eruptions over the past nine centuries. *Int. J. Climatol.* **37**, 4146–4157 (2017).
356. Qian, Q., Jia, X., Wu, R. & Wang, M. Impact of Arctic sea ice interannual variation on nonmonsoonal winter precipitation over the Eurasian continent. *J. Clim.* **36**, 4619–4634 (2023).
357. Brönimann, S. et al. Last phase of the Little Ice Age forced by volcanic eruptions. *Nat. Geosci.* **12**, 650–656 (2019).
358. Dätwyler, C., Grosjean, M., Steiger, N. J. & Neukom, R. Teleconnection and relationship between the El Niño–Southern Oscillation (ENSO) and the Southern Annular Mode (SAM) in reconstructions and models over the past millennium. *Clim. Past* **16**, 743–756 (2020).

359. Li, J. et al. El Niño modulations over the past seven centuries. *Nat. Clim. Change* **3**, 822–826 (2013).
360. Zhu, F. et al. A re-appraisal of the ENSO response to volcanism with paleoclimate data assimilation. *Nat. Commun.* **13**, 747 (2022).
361. Pausata, F. S. R., Karamperidou, C., Caballero, R. & Battisti, D. S. ENSI response to high latitude volcanic eruptions in the Northern Hemisphere: the role of the initial conditions. *Geophys. Res. Lett.* **43**, 8694–8702 (2016).
362. Deng, J. & Dai, A. Arctic sea ice–air interactions weaken El Niño–Southern Oscillation. *Sci. Adv.* **10**, eadk3990 (2024).
363. Pervez, M. & Henebry, G. Projections of the Ganges–Brahmaputra precipitation: downscaled from GCM predictors. *J. Hydrol.* **517**, 120–134 (2014).
364. D'Agostino, R. & Timmreck, C. Sensitivity of regional monsoons to idealised equatorial volcanic eruption of different sulfur emission strengths. *Environ. Res. Lett.* **17**, 054001 (2022).
365. Kondrashov, D., Feliks, Y. & Ghil, M. Oscillatory modes of extended Nile River records (A.D. 622–1922). *Geophys. Res. Lett.* **32**, L10702 (2005).
366. Wang, G. & Eltahir, E. A. B. Use of ENSO information in medium- and long-range forecasting of the Nile Floods. *J. Clim.* **12**, 1726–1737 (1999).
367. Zaroug, M. A. H., Eltahir, E. A. B. & Giorgi, F. Droughts and floods over the upper catchment of the Blue Nile and their connections to the timing of El Niño and La Niña events. *Hydrol. Earth Syst. Sci.* **18**, 1239–1249 (2014).
368. Melesse, M. B. & Demissie, Y. Hydrology and droughts in the Nile: review of key findings and implications. *Water* **16**, 2521 (2024).
369. Cheng et al. Influence of winter Arctic sea ice anomalies on the following autumn Indian Ocean Dipole development. *J. Clim.* **38**, 3109–3129 (2025).
370. Kim, H., Villarini, G., Yang, W. & Vecchi, G. Global response of floods to tropical explosive volcanic eruptions. *Nat. Geosci.* **18**, 983–988 (2025).
371. Pedersen, R. A. et al. The impact of regional Arctic Sea ice loss on atmospheric circulation and the NAO. *J. Clim.* **29**, 889–902 (2016).
372. Zambri, B., Robock, A., Mills, M. J. & Schmidt, A. Modelling the 1783–1784 Laki eruption in Iceland: 1. aerosol evolution and global stratospheric circulation impacts. *J. Geophys. Res. Atmos.* **124**, 6750–6769 (2019).
373. Butler, A. H., Sjoberg, J. P., Seidel, D. J. & Rosenlof, K. H. A sudden stratospheric warming compendium. *Earth Syst. Sci. Data* **9**, 63–76 (2017).
374. Zhang, C., Zhang, J., Maycock, A. C. & Tian, W. Distinct tropospheric anomalies during sudden stratospheric warming events accompanied by strong and weak Ural Ridge. *npj Clim. Atmos. Sci.* **7**, 280 (2024).
375. Briffa, K. R. et al. Reassessing the evidence for tree-growth and inferred temperature change during the Common Era in Yamalia, northwest Siberia. *Quat. Sci. Rev.* **72**, 83–107 (2013).
376. Oman, L., Robock, A., Stenchikov, G. L. & Thordarson, T. High-latitude eruptions case shadow over the African monsoon and the flow of the Nile. *Geophys. Res. Lett.* **33**, L18711 (2006).
377. Wu, B. & Li, Z. Possible impacts of anomalous Arctic Sea ice melting on summer atmosphere. *Int. J. Climatol.* **42**, 1818–1827 (2022).
378. Zhang, X. et al. Volcanic eruption disrupt ENSO teleconnections with land summer temperature. *Nat. Commun.* **16**, 9882 (2025).
379. Hodell, D. A. et al. Climate change on the Yucatan Peninsula during the Little Ice Age. *Quat. Res.* **63**, 109–121 (2005).
380. Travis-Taylor, L. et al. Last glacial climate variability in the Yucatan Peninsula not just driven by ITCZ shifts. *Commun. Earth Environ.* **6**, 14356 (2023).
381. Travis-Taylor, L. et al. Hydroclimate variability in the northern Caribbean during the last deglaciation was modulated by large-scale atmospheric circulation and climate events. *Commun. Earth Environ.* **6**, 498 (2025).
382. Justino, F., Bromwich, D. H. & Gurjao, C. Atmospheric rivers as mediators between climate teleconnections and burned area variability in North America. *Commun. Earth Environ.* **7**, 99 (2026).
383. Cohen, J. et al. *Arctic change and possible influence on mid-latitude climate and weather* A US CLIVAR White Paper (US CLIVAR Project Office, 2018).
384. Scott, M. Is Arctic sea ice loss changing weather? *National Snow and Ice Data Center* https://nsidc.org/learn/ask-scientist/declining-sea-ice-changing-atmosphere#anchor-clarity-consumed-by-complications (2023).
385. Liu, F. et al. Tropical volcanism enhanced the East Asian summer monsoon during the last millennium. *Nat. Commun.* **13**, 3429 (2022).
386. Li et al. Positive connection between declining Barents Sea ice and interdecadal increasing northeast China precipitation in May. *Int. J. Clim.* **41**, 6270–6282 (2021).
387. Zhou, B. et al. Interdecadal change in the linkage of early summer sea ice in the Barents Sea to the variability of West China Autumn Rain. *Atmos. Res.* **287**, 196717 (2023).
388. Massicotte, P. & South, A. World map. *Natural Earth* https://CRAN.R-project.org/package=rnaturalearth.
389. Wang, D. Volcanic imprints in last-millennium land summer temperatures in the circum–North Atlantic area. *J. Clim.* **36**, 5923–5939 (2023).
390. Esper, J., Frank, D., Verstege, A., Luterbacher, J. & Xoplaki, E. Long-term drought severity variations in 911 Morocco. *Geophys. Res. Lett.* **34**, L17702 (2007).
391. Wurtzel, J. B. Mechanisms of southern Caribbean SST variability over the last two millennia. *Geophys. Res. Lett.* **40**, 5954–5958 (2013).
392. McCabe-Glynn, S. et al. Variable North Pacific influence on drought in southwestern North America since AD 854. *Nat. Geosci.* **6**, 617–621 (2013).
393. Wallace, E. J. Intense hurricane activity over the past 1500 years at South Andros Island, the Bahamas. *Paleoceanogr. Paleoclimatol.* **34**, 1761–1783 (2019).
394. Wang, J. et al. Internal and external forcing of multidecadal Atlantic climate variability over the past 1,200 years. *Nat. Geosci.* **10**, 512–517 (2017).
395. Scroxton, N. et al. Hemispherically in-phase precipitation variability over the last 1700. *Quat. Sci. Rev.* **164**, 25–36 (2017).
396. Trouet, V. et al. Persistent positive North Atlantic oscillation mode dominated the Medieval Climate Anomaly. *Science* **324**, 78–80 (2009).
397. Cook, R. C. et al. A Euro-Mediterranean tree-ring reconstruction of the winter NAO index since 910 C.E. *Clim. Dyn.* **53**, 1567–1580 (2019).
398. Baker, A., Hellstrom, J. C., Kelly, B. F., Mariethoz, G. & Trouet, V. A composite annual-resolution stalagmite record of North Atlantic climate over the last three millennia. *Sci. Rep.* **5**, 10307 (2015).
399. Halfar, J. et al. Arctic sea-ice decline archived by multicentury annual-resolution record from crustose coralline algal proxy. *Proc. Natl Acad. Sci. USA* **110**, 19737–19741 (2013).
400. The North Atlantic Oscillation. *UK Met Office* https://www.metoffice.gov.uk/research/climate/seasonal-to-decadal/gpc-outlooks/ens-mean/nao-description.
401. Nakamura, T. et al. A negative phase shift of the winter AO/NAO due to the recent Arctic sea-ice reduction in late autumn. *J. Geophys. Res. Atmos.* **10**, 3209–3227 (2015).
402. Freitas, A., Bernardino, M. & Guedes Soares, C. The influence of the Arctic Oscillation on North Atlantic wind and wave climate by the end of the 21st century. *Ocean Eng.* **246**, 110634 (2022).
403. Wang, X. & Zhao, J. Trends and oscillations in arctic Mediterranean atmospheric static stability during recent arctic warming. *npj Clim. Atmos. Sci.* **7**, 27 (2024).

Acknowledgements We would like to thank U. Bieber, S. Espeel, C. Mauch, T. Nester, A. Panin, L. Roald, M. Toohey, F. Segura Urra and R. J. S. Wilson for scientific advice. The work was supported by the ERC Advanced Grant 'FloodChange' project (no. 291152), EVISEGURA Project (22670/PI/24), ADAPTAMED Project (PID2024-157662OB-C), Freigeist Fellowship 'The Dantean Anomaly 1309–21', UAntwerp project (BOF FFP230254), German State Project DEMUR (DFG, SPP 2361) and the ECCOREV CNRS (France; consortium no. 3098).

Author contributions A.K., G. Blöschl and A.V. designed the study, interpreted results and wrote the first draft of the paper. A.K. organized, developed and managed the database including supplementary data and information files; A.K. and G. Blöschl took the lead in revising the paper drafts. A.V., G. Blöschl and A.K. were mainly responsible for the statistical analysis. A.K., M. Barriendos, S.E., M. Bauch, N. Maughan, K.D., A.O., J.B., L.E., K.P., I.T., T.S., D.R., M.D., L.S. and O.W. participated in the development of the 1341–1343 flood, weather (documentary and natural proxy) and impact databases, source interpretation and analysis, and the water level and return period estimations. A.K., M. Barriendos, S.E., R.B., I.A., J.B., O.B., G. Benito, C.B., D. Camuffo, D. Coeur, G.D., R.D., L.E., R.G., N. Macdonald, H.P., C.R., P.S.-F. and W.H.J.T. contributed to the 700-year European historical flood database. A.K., A.V., M. Bertola and G. Blöschl carried out the comparison of the 1341–1343 floods and the Pan-European flood database; J.P., M. Bertola and J.K. assisted in data processing and interpretation. All authors interpreted results, and contributed to framing and revising the paper.

Funding Open access funding provided by TU Wien (TUW).

Competing interests The authors declare no competing interests.

Additional information

Supplementary information The online version contains supplementary material available at https://doi.org/10.1038/s41586-026-10888-8.

Correspondence and requests for materials should be addressed to Andrea Kiss or Günter Blöschl.

Peer review information *Nature* thanks the anonymous reviewers for their contribution to the peer review of this work.

Reprints and permissions information is available at http://www.nature.com/reprints.

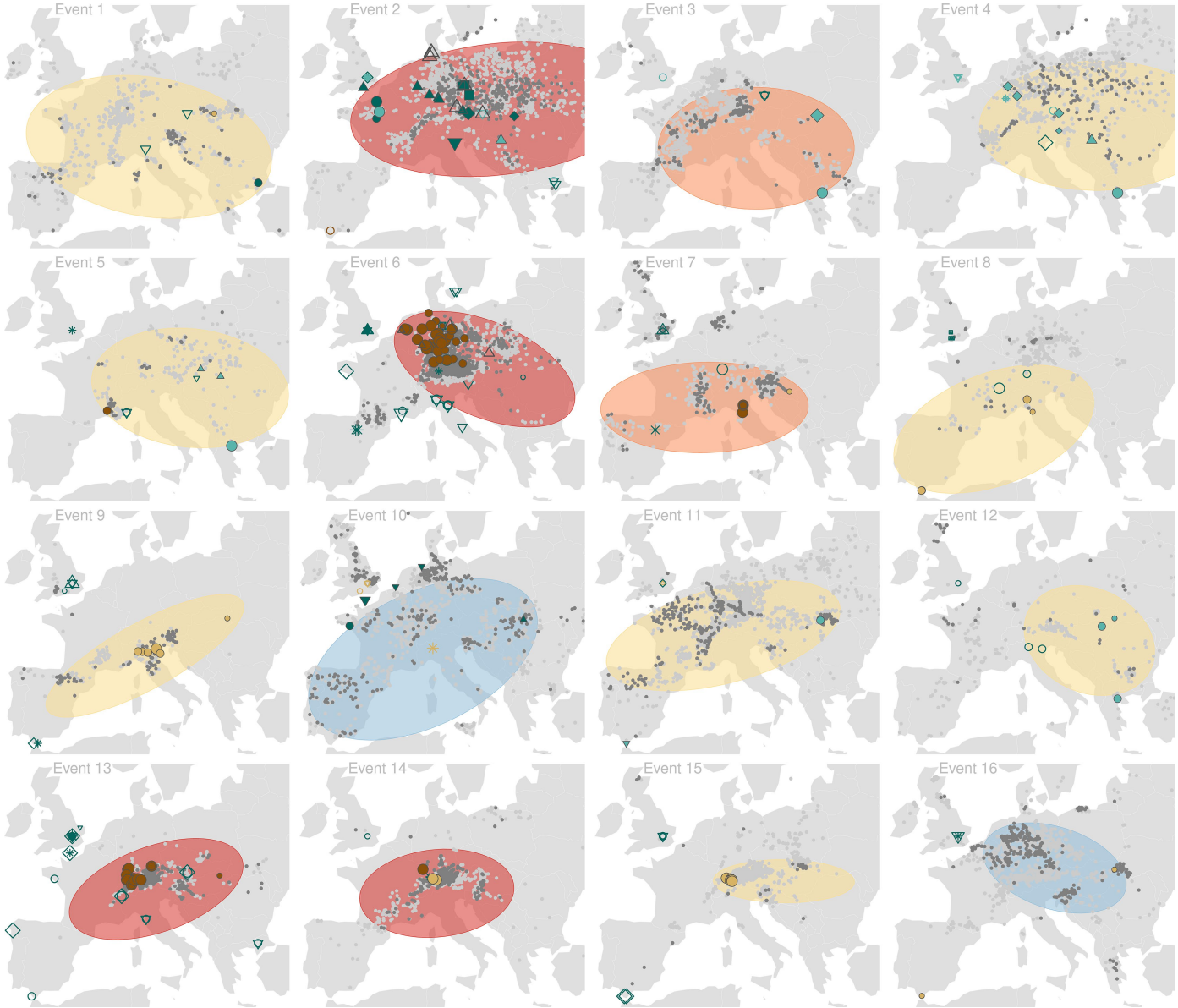

Extended Data Fig. 1 | Conceptual reconstruction of the 1342–1343 floods in Europe. 16 events rendered as ellipses based on historical evidence on floods (161 data points) and meteorological conditions (>217 data points), and on modern analogue events for spatial extent (see Methods section, Supplementary Data 1, 2, 4, 6).

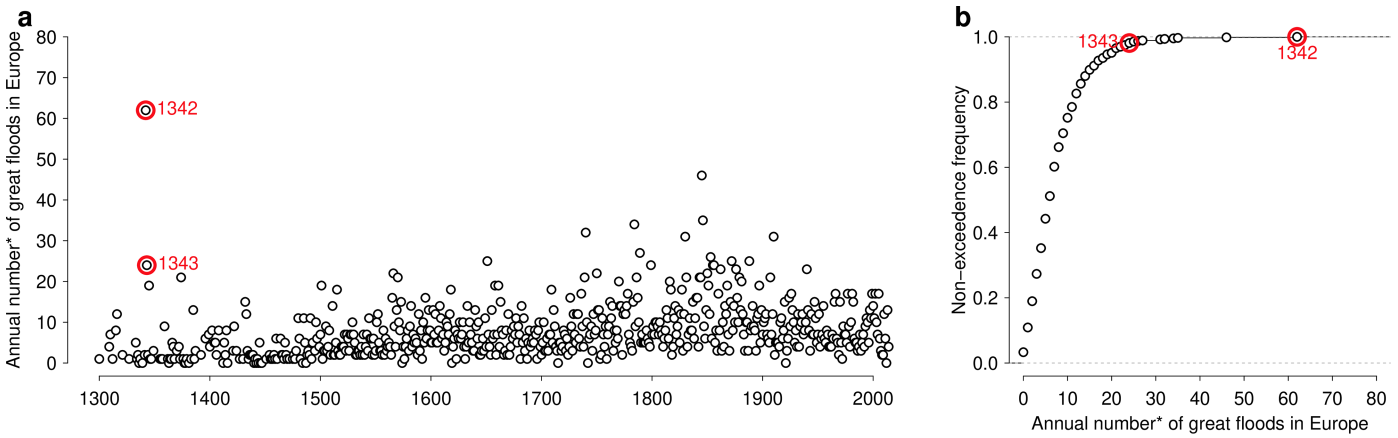

Extended Data Fig. 2 | Annual frequency of great and extraordinary floods in Europe in the last 700 years. Original data without bias correction (*). Source of data: Supplementary Table 4.

Extended Data Table 1 | Overview of major floods and main causes between late 1341 and late 1342 compared to similar modern flood events in the period 1960–2020 (events 8–16)

Late 1341-1342 floods			Probable flood analogues			Similarities and differences
Event number, Timing, Return period	**Documented extension** (on an 'at least' basis)	**Mechanisms**	**Timing**	**Documented extension** (on an 'at least' basis)	**Mechanisms**	
1) Mid-November - December 1341 T=20-50	SE-Slovakia, NE-Greece (W-Turkey, S-Bulgaria)	(heavy) prolonged rains (+snowmelt) *(convective)*	Late December 2009-January 2010	E-Slovakia, W-Ukraine, NE-Hungary, N-Greece, W-Turkey, Bulgaria, N-Macedonia, N- and C Italy	Rainy Nov., Mediterranean cyclonic activity; late Dec. snowfall melted in the following milder weather	**Similarities**: caused by heavy rains and intense cyclonic activity after prolonged wet weather in the same area. **Differences**: 1341 flood starts two weeks later; known spatial extent of 2010 flood is larger, maybe because the full spatial extent of the Dec. 1341 is unknown
2) Early and mid-February, early March 1342 Candlemas T= 500-1000	N- and partly Central-France, Germany, Czechia, Austria, Slovakia, (Hungary), (great sea surge: Venice)	Snowmelt, rainfall, ice jams (precondition: hard winter with much snow/ rain, then mild SW winds	(Mid-) March-(early) April 2006	France, Belgium, Germany, Czechia, Austria, Slovakia, Hungary, Bulgaria, N-Greece, W-Turkey	Snowmelt, ice jamming, rainfall	**Similarities**: hard, snowy/rainy winter, followed by mild/wet air masses from W-SW causing rapid melting, ice jamming. **Differences**: 1342 flood is more intense; 2006 affected S-France; no sea surge in Venice in 2006
3) March 1342 T=50-100	N-Greece, NE-Hungary (*SW-Ukraine; S-Germany*)	Heavy rains (*+snowmelt* after snowy winter) *convective*	(Mid-) March-(early) April 2006		Snowmelt, ice jamming, rainfall	**Similarities**: the flood happened after hard, snowy winter followed by heavy rainfall. **Differences**: in 2006 the Balkan flood starts earlier
4) April 1342 T=20-50	(S-)Germany, (Austria,) Slovakia, (*Hungary, N-Croatia*,) N-Serbia, N-Greece	(*Snowmelt +rain*)	(March-) May 2006	Hungary, Slovakia, W-Romania, N-Serbia, N-Croatia, Bulgaria, N-Greece, W-Turkey	Late snowmelt, rainfall	**Similarities**: in both cases, Central Europe and the Balkan were affected. Floods were caused by snowmelt and rain – after three winter-spring flood waves. **Differences**: greater extension in 1342, areas repeatedly affected
5) (Early/ mid-)May 1342 T=10-50	W-Slovakia, E-Hungary, N-Greece	*(Rainfall*)	Late April (-early May) 1995	E-Germany, Czechia, E-Austria, E-Sweden, S-Norway, S-Finland, Estonia, W-Ukraine, Hungary, Serbia	Wet winter/ spring resulted in oversaturated soils, followed by heavy rains	**Similarities**: N-Greece and the Carpathian Basin are affected (Axios+Tisza); intense Mediterranean cyclonic activity in winter; wet early/mid spring followed by heavy rainfall events in May. **Differences**: reported European extent of 1995 flood is much greater (1342: data shortage)
6) Late July-early August 1342 Magdalena T=1000	Germany, (E-/SE-France?), Netherlands, Austria	8-day (*10,000-year*) heavy rainfall (low-pressure cond. in July over W-, N-Alps, after very wet winter, spring, summer)	June 2013	France, Germany, Czechia, Poland, Austria, Hungary, Serbia, Romania, Bulgaria	Wet winter/spring, torrential rains, wet antecedent conditions	**Similarities**: more than one slow-storm system; preceding wet conditions are followed by outstanding heavy rainfall (lasting for a few days) and flash floods; relatively restricted spatial extension. **Differences**: in 1342 the summer flood wave spatially more to W-NW; preceding prolonged low-pressure system (?)
7) Late August 1342 T=50-100	(N-)Italy, (*SW-Hungary – SE-Austria*)	Much/heavy rains; wet antecedent weather conditions*; convective*	October 1993	UK, France, SE-Germany, N-Spain, N-Italy, W-Hungary, SE-Austria,Slovakia, Serbia, BIH, Croatia	Heavy rainfall	**Similarities**: caused by heavy rainfall (Mediterranean cyclone activity). **Differences**: difference in season and flood intensity; part of a spatially, temporarily more extensi-ve (less intense) European event

Brackets indicate presumed (but not directly mentioned) information based on the sources. T is the estimated return period (yrs). Italics indicates higher uncertainty.

Extended Data Table 2 | Overview of major floods and main causes between late 1342 and late 1343 compared to similar modern flood events in the period 1960–2020 (events 8–16)

Late 1342-1343 floods			Probable flood analogues			Similarities and differences
Event number, Timing, Return period	**Documented extension** (on an 'at least' basis)	**Mechanisms**	**Timing**	**Documented extension** (on an 'at least' basis)	**Mechanisms**	
8) (Mid-) October 1342 T=20-100	(*SE-, N-*) Spain, N-Italy	Rain floods/ torrential waters; *convective*	October 1960	UK, E-Spain, S- and C-France, E-Germany, N-Italy, E-Austria, W-Ukraine, E-Slovakia, W-Croatia	Heavy rain	**Similarities**: heavy rains and storms caused extensive flooding over the Western and Central Mediterranean. **Differences**: In 1342, no data is available on floods in the Carpathian Basin and in France; known spatial extension in 1960 is greater, but lower intensity
9) (Mid-) November 1342 T=50-100	N-Italy, SE-Slovakia, NW-Ukraine, NE-Hungary	heavy rains; *convective*	October - early November 1966	Spain, N-Italy (great flood in Florence), S-Austria, Slovenia, SW-Hungary	Heavy rains caused by intensive cyclone activity	**Similarities**: intense Mediterranean (and related) cyclonic activity; floods caused by heavy rains. **Differences**: flood data only from the SW-Carpathian Basin
10) January-(mid-) February 1343 T=10-50	NE-Hungary (SW-Ukraine); *E-Slovakia & N-Romania*; major sea surge: S-UK, N-France, Spain; *Netherlands*	Prolonged rains (Dec., Jan.) in NW-France; *p. sea surge in the Netherlands; rainy winter: S-Spain*)	(Mid-January-) February 1979	Spain, France, Portugal, E-Anglia, W-Germany, Hungary, Serbia, W-Ukraine, N-Switzerland, Bulgaria, W-Turkey, N-Greece		**Similarities**: Atlantic coastline and EC-Europe both affected; frosts and snow (with strong W, NW winds) in (SE-)England; roughly similar intensity. **Differences**: in 1979 more flood reports in Western and C-Eu (i.e. larger spatial coverage)
11) (Early/mid-) April 1343 T=20-100	SE-Spain, E-Hungary (W-Romania, SW Ukraine)	Heavy rains, storm (*cyclone*)	March 2001	S-England, Spain, France, Netherlands, Germany, Czechia, Austria, Lithuania, W-Russia, Belarus, Slovakia, Hungary, Bulgaria, Croatia	After wet winter/early spring, heavy rains caused by Mediterranean cyclonic activity	**Similarities**: flood generation, wet antecedent conditions; both Spain Carpathian Basin affected. **Differences**: known European extension of the event is larger in 2001; the magnitude of the 1343 event was larger (data shortage?)
12) Early/ mid-May 1343 T=20-50	(N-Macedonia) N-Greece, E-Hungary, W-Ukraine	Wet winter and spring, superposed by abundant rainfall	Apr-May 2000	Norway, S-Sweden, Scotland, N-Italy, Austria, Poland, Romania, Belarus, Ukraine, S-Finland, Estonia, Serbia, Bulgaria, N-Greece, W-Turkey, Hungary, Slovakia, C-Spain, Croatia, Czechia	Wet winter and spring, superposed by abundant rainfall, Mediterranean cyclonic activity	**Similarities**: timing and synchronicity between the Carpathian Basin and the Balkan. **Differences**: much larger known spatial extent in 2000, but probable higher flood intensity in 1343.
13) Late July-early(/mid-) August 1343 Jacob T=100-200	(W?-, N-, C-, E-) Switzerland, E-France, S-Germany, N-Italy *C-Transylvania*; mid-July: NE-Hungary (SE-Slovakia)	Heavy rains, abundant, prolonged rainfall, wet spring-summer *likely Vb*	August 2005	W-, C-Switzerland, E-France, S-Germany, N-Italy, C-Romania, Slovakia, Hungary	major Vb event with antecedent wet conditions; extreme rainfall over N-Alps	**Similarities**: timing; both were Vb events; at least 100-year return period, caused by heavy rains, wet antecedent conditions. **Differences**: the event 1343 was greater in magnitude
14) late August–early September 1343 Bartholomew T=500-1000	S-Germany, NE-, E-Switzerland, W-Austria, E-France, *C-Transylvania*	Heavy rains *likely Vb*	May 1999	France, Germany, Switzerland, Austria, Hungary, Finland, Belarus	incessant rains, wet preconditions	**Similarities**: incessant heavy rains over the (N-)Alps. **Differences**: in 1343 no contemporary data in Germany, Austria, East C-Eu, only a 'fear of flood' report in C-Transylvania
15) Mid-September 1343 T=50-100	Lake Constance area (S-Germany, N-Switzerland)	Incessant rains *convective*	September 1984	S-UK, Germany, N-Switzerland, Austria, Slovakia, W-Hungary, Croatia, Poland, W-Ukraine	incessant rains around Lake Constance as part of cyclonic activity in C-Eu	**Similarities**: incessant rains (days) caused extensive flooding. **Differences**: known spatial extension of the 1984 event is much larger (data shortage in 1343?)
16) Mid-October 1343 T=10-100	W-Ukraine, NE-Hungary	(Abundant rainfall)	November 1998	Croatia, Czechia, France, Germany, Switzerland, W-Ukraine, Hungary	wet air masses from the Mediterranean (Genova low pressure system)	**Similarities**: (most probably) caused by Mediterranean cyclonic activity. **Differences**: known spatial extent is much larger in 1998 (maybe related to the lack of data)

Brackets indicate presumed (but not directly mentioned) information based on the sources. T is the estimated return period (yrs). Italics indicates higher uncertainty. Vb indicates cyclones originating near the western Mediterranean or Gulf of Genoa and moving northeastward across northern Italy toward central Europe, turning counterclockwise[159].

Extended Data Table 3 | Long-term changes caused by the 1342–2343 floods (infrastructural innovations, strategies and new flood protection and mitigation design after the 1342–1343 events)

I) New/stronger dykes, dyke systems, river regulation, flood protection measures	a) New and/or stronger dykes (e.g. Rhine delta, Flanders; sometimes also in areas without direct flood reports e.g. Vistula-Nogat) b) River regulation, canal reparations, improvements for flood prevention (Danube at Oberaltaich, Bologna) c) New flood protection and mitigation measures, regulations, agreements: more organised, systematic flood protection, mitigation, prevention system can be traced in Europe even in areas without direct flood reports (e.g. Würzburg, Säckingen, Prague)
II) Bridge (re-) building, improvement activities in Europe	a) Rebuilding of bridges; sudden increase in the number of bridges in following years b) More, massive stone structure (multicausal), technological innovations (e.g. Prague)
III) Reorganisation of urban space, modification of urban design	a) Systematic reorganisation of town and riverine area, (multifunctional) buildings, infrastructure, improving multifunctional shoreline buildings, towers (e.g. High-Rhine area: Säckingen, Prague) b) Bigger, stronger (multifunctional) town walls, additional walls in the city – instead of/over the town walls damaged by the floods (e.g. Strasbourg) c) Potential shift of importance in public space to flood-free mainland location (from island town centre: Säckingen, Frankfurt)
IV) Raising public awareness: objects, processes and regulations in urban space	a) Scientific and high-status discussions, raising awareness for “climate change” and flood change and their obvious physical connections, health issues (e.g. Sorbonne/Paris, Kalocsa) b) Future warning: flood marks/memory stones as public reminder, spatial memory, determination of flood-prone areas in urban space (e.g. Frankfurt, Würzburg); religious (memory) objects (e.g. Göttingen Cross); flood procession repeatedly marking flood extension (Frankfurt) – raised awareness and helped better local and town planning

References; see Supplementary Data 3; an extended version of the table with original source text quotations on damages is available in Supplementary Information 2.

Extended Data Table 4 | Socio-economic impact groups of the great weather and flood anomalies of 1342–1343

Major impact groups as in Fig. 3	Impact types included in impact groups as in Supplementary Table 3
Social tension, military, spiritual & scientific impacts/response	Spiritual response (e.g. biblical notes/connotations, organised prayers, processions, dedications) to extreme rains and floods, astronomy notes (e.g. a. reasoning of extreme floods), fear (emotional/psychological impacts), flood marks/memorials, accusation/scapegoating (e.g. Jews, high-class/political figures), legal problems (e.g. obstructed land surveys), taxation problems – tax reliefs
Food shortage, famine, disease medical/health issues	Famine, diseases/illness (incl. mental illness) as a consequence of stress due to excess rainfall, floods and consequent dearth
Settlements, buildings demolished; material damages	Houses, mills, town walls, settlements, ships, wine, goods damaged or completely destroyed; major fires
Great infrastructural & related damages, changes	Bridges, roads, dykes destroyed by flood, (new) flood protection objects initiated
Great agricultural & land damage	Islands, harvest, trees, fishponds destroyed, mass soil/land erosion events by excess rains and floods
Fatalities/casualties, mass loss of animals	Victims, severe injuries (human); (mass)loss of animals as a direct or indirect consequence of floods and excess rainfall

References see Supplementary Data 3.